

D. discoideum Integrate Chemical and Mechanical Signals to Achieve Directional Motility

A thesis presented by
Arhana Chattopadhyay

to

the Faculty of the Committee on Degrees in Chemical and Physical Biology
in partial fulfillment of the requirements
for the degree with honors
of Bachelor of Arts
Harvard College, Cambridge, MA
March 2011

Advisors: Jeremy Gunawardena and Natalie Andrew

Acknowledgements

I would like to thank Dr. Jeremy Gunawardena for the opportunity to work in his lab. His support has allowed me to have one of the most enriching academic experiences of my Harvard experience. Over the past two years, I have learned a great deal from him about how to think about the broader questions of biology.

My post-doc, Dr. Natalie Andrew, has been an incredible mentor and friend to me and really made this project possible. From her, I learned: how to make an experiment work, how to be persistent, how to interpret unexpected results, how to make quick fixes in the face of problems, how to make science fun by making nitrogen bubbles and doing *D. discoideum* interpretive dances. Thank you for invaluable guidance, patience, support, and humor. They have meant so much to me.

I would like to thank Professor Jagesh Shah of Harvard Medical School for allowing me to use his device design for this project.

Thank you to all the members of the Gunawardena lab for their kind support and friendship, and for their feedback on my project.

I would also like to thank Tom Torello and Lisa Fountain. They have made thesis writing (almost) painless and have made CPB an academic home for me at Harvard.

Thank you to the readers who helped me with my thesis drafts: Karolina Maciag, Albert Yeh, Joseph Dexter, and Amit Srivastava.

Thank you to my blockmates, friends, and tutors in Dunster House (and honorary Dunsterites)—you are the best people anyone could ever ask for. Thank you especially for your understanding during this hectic time.

And finally, my family. Thank you so much for everything, but most of all, for always believing in me on my journey through life. Your faith, love, and support made this endeavor possible.

Statement of Research

This project was conceptualized, designed, and carried out by Arhana Chattopadhyay with assistance from Natalie Andrew and Jeremy Gunawardena. Arhana learned how to design and fabricate microfluidic devices in spring and summer 2009. The concept of the project was devised in fall 2009 while Arhana pursued lab work in Physics 91r.

Arhana Chattopadhyay conducted all methods, experiments, and data analysis with guidance from Natalie Andrew from fall 2009 through spring 2011. Interpretation of results was a collaborative effort among Arhana Chattopadhyay, Natalie Andrew, and Jeremy Gunawardena in spring 2011. Arhana will be continuing this work through summer 2011.

Abstract

Little is known about how cells process mechanical cues from the environment, and less is known about how these cues are processed in the presence of simultaneous chemical cues. Using a microfluidic device, *Dictyostelium discoideum* cells were exposed to chemical gradients and orthogonally directed shear stress simultaneously. Time-lapse imaging of cells experiencing combined stimuli of 3 different chemical gradient regimes and 3 different flow regimes revealed: 1) cells directionally integrate the stimuli rather than switching between cues; 2) increasing the mechanical signal *but not the chemical signal* impacts the cell's direction. These findings support a selective rather than instructive model of cell motility in the presence of multiple directional cues.

Useful definitions

cAMP- 3'-5'-cyclic adenosine monophosphate, chemoattractant for *D. discoideum*

Chemotaxis- movement in response to a gradient of a diffusible chemical signal

Developed cells- long, polarized cells that are under starvation conditions and are chemotaxis-competent

Dunn chamber- commonly used non-microfluidic platform for studying chemotaxis

Laminar flow- streams of fluid flow in a parallel manner

Mechanotaxis- movement due to applied force

PDMS- polydimethylsiloxane, an optically clear, porous, and biocompatible polymer used to fabricate microfluidic devices

Shear stress- force that is applied parallel rather than normal to the surface of the cell

Vegetative cells- round cells that feed on *E. coli*, chemotax toward folate, move randomly, and exist as single cells

I. Background

1. Eukaryotic cells migrate in response to chemical signals and mechanical interactions with the environment

Motility is essential to many eukaryotic cell functions. For example, carefully coordinated cell movement is required in processes as diverse as wound healing, cell division, the immune response, tumor metastasis, and embryogenesis (King and Insall, 2009). This coordination is commonly achieved through chemical signaling.

Chemotaxis is the ability for cells to sense and move up an external gradient of a diffusible chemical signal (King and Insall, 2009). Engelmann discovered chemotaxis in bacteria in 1881 (Berg and Tedesco, 1975). It was later discovered that certain eukaryotic cells, like neutrophils, epithelial cells, cancer cells, and the soil-dwelling amoeba *Dictyostelium discoideum*, also chemotax. Moreover, mutant analysis has revealed that the pathways governing eukaryotic chemotaxis are largely conserved across organisms (Bagorda *et al.*, 2006).

In prokaryotic chemotaxis, the signaling pathways are short and decision-making processes are simple. Eukaryotes, however, are much larger and more complex than prokaryotes, and eukaryotic cell migration still contains several open questions. Although significant progress has been made in parsing the mechanisms of cell migration through studies of mutant phenotypes, there is no single consensus about how these mechanisms couple for movement systematically. For example, it was for many years believed that eukaryotic cells utilize *spatial sensing*

during chemotaxis, in which they sense a gradient by measuring the concentration difference at two points in the gradient simultaneously, rather than sequentially. However, studies have shown that eukaryotic cells may instead employ *temporal sensing*, in which they iteratively reevaluate the direction of the strongest chemical signal and move towards it, much like bacteria do (Parent *et al.*, 1999; Andrew and Insall, 2007; Bosgraaf *et al.*, 2009a).

Furthermore, an emerging view is that cell migration is even much more complex than chemotaxis may indicate. For example, it is necessary for chemotaxing cells to navigate different types of mechanical environments. When migrating towards a chemoattractant signal, neutrophils must be able to migrate along blood vessel walls and through epithelial gap junctions into the extracellular matrix of cells of virtually any organ in the body (Jannat *et al.*, 2010). Migrating cells such as epithelial cells, fibroblasts, and neutrophils have all been shown to respond to the stiffness of the substrate on which they crawl (Discher *et al.*, 2005; Jannat *et al.*, 2010). Further, Décavé *et al.* (2003) recently found that *D. discoideum* cells crawl directionally in response to fluid flow in a process called mechanotaxis. Therefore, while eukaryotic chemotaxis remains an active area of research, it is critical to understand that chemoattractants are only part of a host of signals that a cell must respond to during migration. In this work, I offer clues about how one model organism, the eukaryotic amoeba *Dictyostelium discoideum*, processes simultaneous chemical and mechanical cues.

2. *D. discoideum* is a model organism for eukaryotic chemotaxis

While studying mammalian cells has clear relevance to physiology, the complexity of mammalian cells often precludes the asking of simple questions. An ideal candidate to study eukaryotic chemotaxis is the unicellular, soil-dwelling amoeba *Dictyostelium discoideum*, which is simpler than mammalian cells yet conserves many key mammalian-cell chemotaxis pathways. A major experimental advantage of this model organism is that it is relatively straightforward to maintain at 25°C, with a population doubling time of eight hours. Another benefit is that it is genetically tractable, with a small, compact, haploid genome. A third advantage is the existence of an extensive and readily available library of mutants that have been developed for various studies over the past fifty years (Kessin, 2001; King and Insall, 2009).

D. discoideum cells exhibit persistent random motion, in which they crawl in the absence of any guidance cues (King and Insall, 2009; Satulovsky *et al.*, 2008). They do this by extending pseudopodia, protrusions of polymerized actin, which establish the speed, direction, and trajectory of movement (Van Haastert, 2010). When an *E. coli* food source is available, *D. discoideum* cells are in a vegetative state and chemotax towards folate secreted by the bacteria. When starved, however, they are in a developing state and secrete waves of cyclic adenosine monophosphate (cAMP) as a survival mechanism. Neighboring cells respond by chemotaxing towards the source of cAMP, and they propagate the signal by secreting their own cAMP. Cells are approximately 10 µm in length and can sense a concentration difference of as little as 2% from front to back. The cells then begin streaming, or aggregating, to eventually form fruiting bodies. The fruiting bodies consist of a stalk

holding up a ball of cells, a conformation that allows cells to conserve energy given a scarce food supply and also increases the likelihood of dispersal of cells to new sites with available food sources (Kessin, 2001; King and Insall, 2009).

Developed *D. discoideum* responding to a cAMP signal are often used for chemotaxis studies; traditionally, cells are stimulated with cAMP using a micropipette held a short distance away, or they are placed in a device that contains a gradient of cAMP, such as a Dunn, Zigmond, or Boyden chamber (Andrew and Insall, 2007; Zicha *et al.*, 1991). The availability of knockout strains has enabled mutant phenotype analysis to explore the molecular pathways governing *D. discoideum* chemotaxis towards cAMP. At least four signaling pathways have been implicated in affecting a cell's ability to sense a chemical signal, polarize by differentially distributing protein expression, and effectively move towards the signal (Van Haastert, 2010; King and Insall, 2009). However, how these pathways coordinate is still unknown, and no single consensus has been reached on how signal transduction couples to movement.

3. Models of *D. discoideum* directional sensing

Several models have been proposed to explain the mechanism that *D. discoideum* uses to sense and crawl up a gradient. The two overarching possible mechanisms are instructive and selective.

In instructive mechanisms, cells are instructed by a chemical signal to express proteins which cause changes. One long-held instructive model of chemotaxis proposes that a cell measures the concentration of chemoattractants at

two points across the surface of the cell *simultaneously* in order to determine the axis of polarization (Parent and Devreotes, 1999). The cell is akin to a “chemical compass,” in which cells polymerize actin into protrusions closest to the source of chemoattractant, and a rapidly diffusing inhibitor impedes actin polymerization outside of the pseudopod to confine the signal. Lateral pseudopods made *de novo* steer the cell when the source of chemoattractant changes (Bourne and Weiner, 2002). The cell thus instructs the molecular machinery of the cell to respond to a signal—i.e., make a new pseudopod.

Alternatively, a more evolving view is the selective model. Selective models like the random protrusion-informed choice model suggest that in shallow gradients, pseudopods are rarely made *de novo* and instead split from pre-existing pseudopods; cells steer by preserving pseudopods that sample higher concentrations of chemoattractant and by retracting lateral pseudopods that are further from the source of cAMP (Andrew and Insall, 2007). Further studies suggest that pseudopods split consistently in a left-right pattern and retain the overall direction of movement, while *de novo* pseudopods steer cells in new directions (Bosgraaf and Van Haastert, 2009a; Bosgraaf and Van Haastert, 2009b). Thus, in the selective model, the cell is producing pseudopods randomly with the *potential* to exist in several possible states, and the signal serves to bias the direction of movement. In this study, I provide preliminary evidence that cells may also use a selective mechanism during mechanotaxis.

4. Mechanotaxis has been observed in *D. discoideum* and may be linked to chemotaxis

While chemotaxis in *D. discoideum* is well-established, recently, Décavé *et al.* (2003) reported a new type of mechanotaxis they characterized as shear-flow-induced cell motility. Mammalian cells interact with their substrate using cell surface-membrane receptors such as integrins and cadherins (Wang *et al.*, 2009); *D. discoideum* do not possess these receptors, but mutant studies suggest that they may attach to a substrate using hydrophobic and hydrophilic surface receptors (Décavé *et al.*, 2002).

Décavé *et al.* (2002) first sought to identify the mechanism of *D. discoideum* detachment from a substrate by applying a shear stress to the cell. They found that at or above a particular threshold stress of 2.6 Pa, the cells detached from the surface. Below this threshold level, however, cells did not detach from the surface and instead changed their contact angle with the substrate. When actin microtubules were depolymerized using the drug *N*-(3-chlorophenyl)-isopropyl-carbamate (CIPC), the cell detachment rate increased ten-fold. This result implicated cytoskeletal networks in the adhesion of cells to a substrate, rather than simply adhesion receptors.

A follow-up study to investigate these results entailed stimulating vegetative *D. discoideum* cells with varying fluid shear stresses below the detachment threshold (Décavé *et al.*, 2003). It was found that actin polymerization occurs on the side opposite to the zone of maximum stress. This polarization subsequently causes cells to migrate in the direction of actin polymerization, to the side of the cell away

from the shear stress. The study also found a greater number of *de novo* pseudopods were formed in the direction of movement. The molecular mechanisms of this phenomenon are largely unknown; possibilities include the activation of stress-activated ion channels which or protein recruitment to the actin cortex. A possible explanation for this mechanotactic response is that *D. discoideum* cells might have evolved to respond to shear forces in nature such as rain drops and streams.

An intriguing proposal is that the mechanotaxis and chemotaxis signaling mechanisms are linked because cells in which the PI3K pathway (known to be important for chemotaxis) was abrogated, the cells no longer responded to mechanical stimuli. Strikingly, chemotaxis and mechanotaxis have also been linked in neutrophils in a recent study (Jannat *et al.*, 2010). This study reported that the chemotactic index of the cells, or the efficiency of chemotaxis, increased as the surface on which cells were adhered became stiffer. While no molecular basis for this phenomenon was elucidated, this study suggested that the coupling of mechanotaxis and chemotaxis may be important in many cell types.

Thus the complex issue of how cells integrate different types of signals in order to move remains an open question in eukaryotic cells. The focus of this thesis is to investigate the interplay between chemical and mechanical signals in *D. discoideum*, and how cells couple these signals in a coherent way to migrate, with the ultimate future goal of shedding light on common mechanisms shared by motile eukaryotic cells.

5. A microfluidics-based experimental strategy

To approach the problem of studying the interplay between chemotaxis and mechanotaxis, I designed an experiment such that the gradient and the shear stress signals were placed in orthogonal directions. I hypothesized that the population of cells would exhibit one of two behaviors: (1) cells would respond to either the chemical or the mechanical signal; or (2) cells would integrate the signals in some way and respond by moving in a direction that was a combination of these signals—i.e., in a diagonal direction. It is important to note that “integration” in the second case is defined as either a simple superposition of the responses to the two signals or a more complex process occurring in the signal transduction pathway of the cell. A schematic of these hypotheses is shown in figure 1.1. The advantage of this strategy was that it allowed independent observation of the response to each signal.

Traditional techniques for studying chemotaxis include Dunn chamber and micropipette assays. In a Dunn chamber, a gradient is formed by long-range diffusion of cAMP from a source to a sink. In a micropipette assay, a micropipette filled with cAMP is placed adjacent to a cell, and a cAMP gradient is formed by short-range diffusion. However, neither of these assays would allow me to exert a shear stress on the cells—even the Dunn chamber is not tightly sealed and contains no inlets or outlets for generating flow. Therefore, one attractive option is to use microfluidics.

Microfluidic devices are an emerging platform for studying chemotaxis of neutrophils and *D. discoideum* (Song *et al.*, 2006). In microfluidics, the gradient is generated by flow rather than by diffusion from source to a sink, as described in

Protocol Development, and a gradient can be established and maintained with much greater control than traditional techniques. Another advantage is that microfluidics requires a closed, tightly sealed chamber and contains inlets and outlets so that fluid flow can be generated externally. Thus, a microfluidic platform would allow me to precisely modulate both the gradient in the device (by adjusting the starting concentration of cAMP) and the shear stress on the cells (by modulating the flow rate of liquid).

6. Experimental questions

The questions I wished to address were the following:

1. When stimulated with a chemical and mechanical signal, do cells respond to either signal? If so, do they integrate the signals in some way?
2. How do the relative strengths of each signal impact the cell's decision?
3. If indeed cells integrate the signals, at what level does this processing occur?

7. Summary of project

In this project, I accomplished the following:

1. I designed and optimized a microfluidic platform for addressing my experimental questions.
2. I determined that when stimulated with both chemical and mechanical signals, the cell integrates the signals rather than choosing one.
3. I determined that increasing the amplitude of the mechanical signal but not the amplitude chemical signal impacts the cell's direction.

4. I present evidence that a cell's decision to move is selective rather than instructive and is computed at the pseudopod level.

II. Protocol Development

1. Designing the microfluidic device

The first challenge in developing the experimental platform was to create a stable and reproducible linear gradient of cAMP in a microfluidic device.

While non-microfluidic gradient generators rely on diffusion of cAMP from a source to sink of buffer, a microfluidic gradient is generated by flow (Jeon, 2002). Typically at the microfluidic scale, fluid undergoes laminar flow—streams of liquid flow parallel to one another. Diffusive mixing of neighboring streams can occur if flow rate is low enough (Wang, 2008). This principle is the key to the pyramidal gradient generator device that has been previously used to study neutrophil, cancer cell, and *D. discoideum* chemotaxis (Song *et al.*, 2006). The device has two inlets—one for chemoattractant ligand and one for buffer (figure 2.1a). Downstream of these is a hierarchy of serpentine microchannels. Two fluid streams converge to three output channels. Due to laminar flow, one channel carries pure buffer, one channel carries pure ligand, and the central channel (figure 2.1b) is split into equal streams of ligand and buffer. Diffusive mixing is facilitated by the length of the channels and the folding geometry at the corners. This effect is amplified through the levels of the device so that the output of the network is a series of parallel streams of fluid with ratiometrically decreasing concentrations of cAMP (figure 2.1c). Downstream, in the cell chamber, the parallel streams mix diffusively to create a smooth gradient profile. The primary advantage to this design is that it requires only two inputs to create a gradient.

My first attempt to design this gradient generator had several problems (figure 2.2a). I found that the serpentine channels were not long enough to allow enough diffusive mixing between adjacent streams of fluid, and there were too few levels of the serpentine network to create a fine gradation of streams. Likewise, because the cell chamber was short, the streams downstream of the network did not have enough time to diffusively mix. The result was a concentration profile that remained stepped rather than smooth (figure 2.2b). With this profile, it was very likely that some cells would be situated in the middle of a laminar stream and therefore experience a constant concentration of cAMP rather than a front-to-back gradient and thus not move.

I used a microfluidic device design from Jagesh Shah (Harvard Medical School, Boston, MA) for a pyramidal gradient generator for my experiments (figure 2.1a). The design solved many of my earlier problems—the channels were longer, there were a greater number of levels in the serpentine network, and the cell chamber was longer. I used standard microfabrication techniques to make the devices, as detailed in Materials and Methods.

2. Controlling shear stress within the device

The second challenge was to finely control the shear stress due to fluid flow within each device. Common approaches include driving fluid through inlet 1 and inlet 2 independently using a programmable syringe pump (Jeon *et al.*, 2002; Song *et al.*, 2006; Wang *et al.*, 2008). I tried this technique and found that using positive pressure to drive flow through the inlets frequently caused an imbalance between

inlets 1 and 2—a slight differences in amount of gas in the syringe pumps, or in the length and even the height of the tubing connected to the ports, caused a differential in the rates of flow through each inlet. Since the rates of flow through each inlet were different, the first bifurcation at the top of the device was not split equally between the cAMP and buffer streams. The downstream effect was that the gradient pattern in the downstream cell chamber was disrupted. To resolve this imbalance problem, I switched to driving flow using negative pressure, or a vacuum. The guiding principle is that if fluid is pulled through the bottom of the device, then fluid is driven at the same rate from both inlets. Thus fluid flow is automatically balanced. One additional advantage to this technique is that I could simply place a droplet of buffer or cAMP at the entrance of the inlet without inserting a tube into the inlet. I could then switch inputs by rapidly wicking the droplet off the surface of the device and replacing it with a new droplet without disrupting the cells in the chamber.

In order to modulate the flow through the device, I used a vacuum regulator hooked up to the lab vacuum source, which could control the amount of vacuum pressure. I found that I needed even finer gradation of vacuum pressure than the regulator allowed, so I increased the resistance upstream of the vacuum by connecting three conical tubes series using rubber tubing. Each unit of added resistance allowed finer control of the flow rate using the same resolution of control over the vacuum.

At the beginning of each trial, I measured the flow rate of liquid exiting the outlet port at the beginning of each experiment by measuring the length of tubing

the fluid traveled through per three minutes. I took a separate measurement of flow rate during the course of the assay to confirm that it had not changed. In order to ensure that gravity did not impact the flow rate of fluid through the tubing, I taped the tubing to the microscope stage so that the tubing was at the same height as the device. Due to the spatial isotropy of the cell chamber, I assumed that all cells in the device experienced identical shear stress.

In order to convert flow rate to pressure, I used the model formula used by Décavé *et al* to relate shear stress to fluid flow (2003). The model additionally assumes that shear stress is proportional to the hydrodynamic forces experienced by the cell.

$$\sigma = \frac{6\eta J}{WH^2}$$

Where σ = shear stress (Pa) ;

η = dynamic viscosity of cAMP solution ($\sim 10^3$ Pa · s) ;

J = volume flux of fluid ($\frac{\mu\text{L}}{\text{min}}$) ;

W = width of cell chamber (475 μm);

H = height of cell chamber (13 \pm 1 μm).

3. Establishing and verifying the gradient within the device

Ostensibly, the microfabrication process is designed to produce uniform microfluidic devices. However, I found that even with the same process and same design, there is variability from device to device that could impact performance. For example, if there is any resistance-causing blockage in the channels, such as debris

or dust, then the flow rate through that channel is slowed and the gradient in the cell chamber is disrupted. Thus, I verified that a gradient could be formed in each device by flowing a colored food dye through inlet 1 and buffer through inlet 2 before loading the cells and visually inspecting that a gradient formed. In my initial attempts, I used food dye to verify the gradient *after* the cells had been loaded into the device. However, I found that cells rounded up and stopped moving when exposed to the dye. A simple solution that I can try in the future is using a dye with low toxicity for cells, such as fluorescein, to verify the gradient.

Finally, an additional consideration was the influence of high flow rate on the gradient. As mentioned previously, the gradient is formed in the device due to diffusive mixing of laminar streams of fluid in the cell chamber. At very high flow rates, I considered the possibility that less diffusive mixing occurs and the concentration profile could be stepped rather than smooth, as mentioned previously. To check that a stable gradient was formed at even higher flow rates, I measured the gradient across different portions of the cell chamber by imaging a gradient formed from food dye and water. I used Image J image processing software to measure pixel intensity and found that even at vacuum pressures as high as 16 psi, a smooth gradient was formed in the cell chamber (the highest vacuum pressures I used in cell experiments were at most 10 psi). The results of this experiment are shown in figure 2.4.

In order to produce a desired gradient, I divided the initial cAMP concentration by the width of the cell chamber (475 μm). For example, to produce a 10 nM/ μm gradient, I used an initial cAMP concentration of 4.75 μM .

4. Degassing and loading the microfluidic device

The presence of bubbles in the closed microfluidic device presented a series of challenges to preparing the devices for the assay and loading cells into the device. Bubbles render an assay unviable because they block upstream channels, thereby changing the gradient pattern, and if they reach a cell chamber, they sweep out all the cells present. Bubbles were often introduced into the device through the inlets if the droplet above an inlet evaporated. Further, at high vacuum pressures, gas was pulled through the porous PDMS into the channels and created *de novo* bubbles. Finally, once the cells were loaded, and a bubble was somehow introduced into the device, there was no method to eliminate the bubbles without harming the cells due to pressure.

To address these problems, I placed moist Kim Wipes around the device during the assay to increase the humidity of the local environment so that droplet inputs at inlets 1 and 2 would not evaporate rapidly. If an inlet was connected to tubing, switching tubing often introduced bubbles, so I surrounded the inlet with a droplet of buffer while switching tubing. Before the start of each assay, I degassed the entire device to eliminate bubbles an initial attempt to degas the device, filling it with buffer and submerging it in water in a vacuum chamber so that the gas in the porous would be pulled into the surrounding water, was unsuccessful in removing all the bubbles from the inlets. An ultimately successful approach was to fill the entire device with buffer, connect each inlet to tubing attached to a syringe that

contained buffer, and inject buffer through each inlet under microscopic observation.

I then loaded the cells into the device using inlets 3 and 4 (inlets are labeled in figure 2.1a). I first used binder clips to close off fluid flow through the tubing attached to inlets 1 and 2—this created resistance in the upstream portion of the device so that if I pressurized inlet 3 or inlet 4, fluid would flow between only these inlets. I then removed the tubing from inlet 4 and replaced it with a 10 μ L pipette tip filled with cells.

At first I had tried introducing the cells into the device using a syringe. However, I discovered that cells would round up due to pressure from depressing the syringe, and cells would become stuck inside the needle of the syringe, causing a low seeding density. Instead, I inserted a pipette tip into inlet 4 and used negative pressure to pull cells into the cell chamber by very gently pulling the plunger of the syringe connected to inlet 3. I then allowed cells to adhere to the glass substrate for at least 30 minutes before gently removing the pipette tip from inlet 4 and replacing it with tubing connected to the vacuum. I then clipped the tubing connected to inlet 3 and removed the tubing connected to inlets 1 and 2. I placed a droplet of desired cAMP concentration on top of inlet 1 and a droplet of buffer on top of inlet 2.

5. Assay conditions

I considered that the cells might behave differently depending on which stimulus they experienced first—cAMP gradient or shear stress. If I turned the vacuum on and set it to the experimental pressure, the cells would experience shear

first because the device is initially filled with buffer, and it can take two to seven minutes (depending on the vacuum pressure) for cAMP to run through the chamber and for the gradient to be established. If I turned the vacuum on and set it to a very low pressure (below the levels of shear stress that induce mechanotaxis) and only turned the vacuum up to full pressure after the gradient had been established, the cells would experience cAMP gradient before being subjected to the experimental shear stress condition. Therefore, I had to choose one of these two methods for consistency. I decided to use the second method, in which cells were subjected to the cAMP gradient before the shear stress, for three primary reasons.

First, I wanted to ensure that the cells in my device were indeed developed and capable of chemotaxing before subjecting them to a shear stress. I took 60-minute time-lapse recordings starting from when I initiated flow but only began image analysis after 20 minutes (and checking to make sure cells were moving directionally). Second, I observed that under high shear stress, some cells rounded up and did not move until they had adjusted, and then they started moving again. I did not want to introduce an additional cAMP stimulus to these already stressed cells; rather, if the cells were chemotaxing and then experienced a shear stress, they would be required to adjust to one rather than two stimuli at a time. Third, shear stresses tended to cause many of the cells to detach from the substrate, and I wanted to analyze only the cells that had been chemotaxing properly before the shear stress was introduced rather than simply any that stayed attached to the substrate.

III. Results

Studies show that *D. discoideum* migrate in response to mechanical as well as chemical stimuli. Further, there is evidence that the molecular machinery governing mechanotaxis and chemotaxis may be linked. However, the question of how they will respond when stimulated with both signals simultaneously has not been explicitly studied. I thus wished to shed light on how cells process both signals by exposing cells to combinations of cAMP gradient and shear stress and quantitatively characterizing the direction in which they migrated in response.

Controls

1. Developed cells move randomly in the absence of shear stress and chemical gradient

To begin my analysis, I first asked how developed *D. discoideum* cells behave in the absence of chemical and mechanical stimuli in the microfluidic device. It is well-established in the literature that both vegetative and developed cells normally exhibit random, or directionless, motion in a dish of buffered solution that would not be biased in any particular direction (Bosgraaf *et al.*, 2009b). This observation was also confirmed for *D. discoideum* cells inside a microfluidic device (Song *et al.*, 2006). I thus hypothesized that cells would exhibit random, directionless movement within the device. If indeed the cells moved randomly, I also expected the standard deviation of the cells' displacement angles would be large.

To test my hypothesis, I loaded developed cells in buffer and imaged them for 20 minutes in the absence of vacuum pressure. I observed first that most of the cells were adhered as single cells or in small groups of ten or fewer cells. However, there were a few large aggregates of cells consisting of several hundred cells. These aggregates, the precursors to fruiting bodies, were present on the surface of the Petri dishes prior to loading. I analyzed the tracks of individual cells for data analysis because the individual positions of cells in aggregates were impossible to track and plotted the angle of displacement of eleven cells (figure 3.2b).

Individual cells situated far (approximately 100 μm) from the aggregates exhibited random motion with an average angular displacement of 63.42° and a standard deviation of 109.105° . It is visually apparent from the angular displacement plot that cells moved in random directions. However, cells close to the aggregates migrated *directionally* towards the center of the clump. I did not observe cells migrate out of the aggregates. Thus the cells' intrinsic cAMP signaling relay system appeared intact within the device.

This experiment was important first because data from the individual cells served as a negative control for the *directed* motion of cells I discuss in subsequent sections of Results. Second, based on these results, I modified my protocol to pass cells through a filter so that large aggregates of cells would not be loaded into the device. Individual cells seemed more likely to reliably respond to external stimuli than cells near clumps. As a caveat, the interaction of individual cells with pre-formed aggregates serendipitously revealed interesting information, as discussed throughout the Results section.

As a second negative control, I asked how cells in a uniform solution of cAMP within the device would behave. When cells are not exposed to a gradient of cAMP but rather a uniform solution, they exhibit random motion because there is no polarization signal (King and Insall, 2009). I loaded cells suspended in a 1 μM cAMP solution into the device and imaged for 20 minutes. I again observed a difference in the behaviors of cells close to and far from pre-formed aggregates. Individual cells far from the aggregates, like in buffer, exhibited random, directionless motion with a mean angle of 28.35° and a standard deviation of 88.74° (figure 3.1a). Cells close to the aggregates, however, migrated *out* of the clumps, rather than into them, as observed in cells in buffer. This result was unexpected because the cells were not exposed to an external gradient of cAMP. One likely explanation for this behavior is that the center of the aggregate was releasing a cAMP concentration less than 1 μM . Thus an inadvertent gradient was set up between the center and the edge of the aggregate. I later observed the same phenomenon in cells in a uniform solution of cAMP and exposed to shear stress (Results section 2). A time lapse panel of cells shows cells migrating out of aggregation centers when exposed to a uniform solution of 1 μM cAMP (figure 3.2).

From this control experiment, I was able to verify that cells that moved directionally up an external gradient in subsequent experiments because of the gradient, rather than simply due to the presence of cAMP. In the future, I can test the motion of cells exposed to different uniform solutions of cAMP to test if cells move differently based on cAMP receptor-occupancy levels. However, based on the results of this test as well as on the well-established theory that only gradients of

cAMP induce directed motion, I am confident that upward migration is due to chemical gradient.

2. Developed cells respond to shear stress independent of the cAMP receptor

In order to approach the experimental goal of determining the behavior of cells perturbed with chemical and mechanical signals, I first needed to determine a suitable set of parameters for each signal. This section addresses how I decided upon a set of shear stress parameters, and Results section 3 addresses how I set the cAMP gradient parameters.

While Décavé *et al.* observe that cells exhibit directed motility along a shear flow, they observe it in cells that are vegetative (Décavé *et al.*, 2003). Cells exhibit very different behaviors in different stages of development; for example, vegetative cells chemotax in response to folate while developed cells chemotax towards cAMP.

Because my overarching goal was to characterize the response of developed cells to shear stress and cAMP, I first wished to observe mechanotaxis alone in developed cells. Décavé *et al.* characterize the response of developed cells to three regimes of stress below the threshold at which they will detach from the substrate: low (0.5 Pa), medium (0.9 Pa), and high (2.1 Pa). I chose these values as a starting point. I hypothesized that, as previously found in vegetative cells, developed cells would move along the direction of shear stress.

I subjected cells to shear stresses of 0.4 ± 0.1 , 0.8 ± 0.1 , and 2.0 ± 0.1 Pa and found that cells moved highly directionally in the direction of flow in all cases as indicated

in figure 3.1 The next logical question was whether cells were moving due to flow rather than due to an intrinsic mechanism of the cells, or whether they were simply being pushed by flow. Décavé *et al.* proposed that cells moved directionally due to a mechanotactic sensing mechanism rather than being pushed along by flow because for two reasons (2003). First, fluid flow velocity was much higher than cell speed, and cells only moved at fluid velocity if they detached from the surface and were swept away from the field of view. Second, they determined through high-magnification microscopy that cells actively partially detached from and reattached to the surface rather than simply being pushed along.

I also observed that cells only moved with bulk flow when detached from the surface—I noticed that, especially at high shear stresses, groups of cells were swept out of the field of view between adjacent 10-second time-lapse frames. Figure 3.3, however, shows that the average speed of cells increases from medium to high shear stress. This difference in speed led me to question, what happens at higher flow rates? One possibility I considered was that cells were rapidly detaching from the surface but actively reattaching to the substrate when exposed to high shear stress. The time-lapse movies I took at 5x magnification did not provide sufficient resolution to answer this question. Thus this question was one motivation for the analysis of cells at higher magnification found in Results section 8.

Second, I asked how cells would move in a uniform solution of cAMP. This experiment served as an important control because one of my main aims was to determine if the single processing machinery governing mechanotaxis and chemotaxis were linked. I expected that if mechanotaxis was dependent on the

cAMP receptor, I would observe a difference in the behavior of cells experiencing shear stress in buffer versus in uniform cAMP. I subjected the same cells from the previous experiment in the same device to a uniform solution of 0.475 μM and a shear stress of 1.2 ± 0.1 Pa and compared them to the medium shear stress and buffer case. I found that the average angle of displacement did not change ($p=0.21$)—cells moved straight across in the direction of flow (figure 3.1 j and k). This data supported the idea that mechanotaxis is independent of cAMP receptor occupancy.

3. Determining a range of cAMP gradients to test

Next, I sought to establish a range of cAMP gradients over which cells would chemotax in my device. Recent studies done in microfluidic devices have characterized the speed and direction of *D. discoideum* in very precise cAMP gradients and have linked these gradients to estimates of cAMP receptor occupancy on the cell surface; it was found that cells responded to a cAMP gradient in the range of 10^{-3} nM/ μm to 10 nM/ μm , with a maximum chemotactic response to cAMP gradients on the order of 10^{-1} nM/ μm (Song *et al.*, 2006). This data is corroborated by separate estimates made in a Zigmond chamber that a chemotactic response occurs when cells are subjected to a cAMP gradient of 10^{-2} nM/ μm and 0.05 nM/ μm (Varnum and Soll, 1984; Vicker *et al.*, 1984).

To test the hypothesis that the strain of cells I was using would exhibit cAMP sensitivity similar to cells in the literature, I first subjected cells to cAMP gradients of 0.1 nM/ μm , 1 nM/ μm , and 10 nM/ μm using Dunn chamber assays. A Dunn

chamber is a standard tool used for studying *D. discoideum* chemotaxis; it consists of two concentric wells between which a gradient is formed by diffusion of cAMP across a 1 mm channel (Zicha *et al.*, 1991). Cells in a Dunn chamber experience zero shear stress because the gradient is formed by diffusion. Conversely, in a microfluidic device, flow is required to generate the gradient. Thus, the Dunn chamber assays also served as an important control.

I tested the 10 nM/ μ m case first, believing that this would result in poor chemotaxis because this was two orders of magnitude above the optimum range as stated in the literature. However, I observed that cells migrated well in the Dunn chamber in this gradient. I next tested cells at the putative optimal gradient of 0.1 nM/ μ m in a Dunn chamber and found that while they chemotaxed up the external gradient, they also responded to waves of cAMP released by pre-formed aggregates of cells, changing directions after a cAMP wave was released by an aggregate downstream of the external cAMP gradient as far away as $\sim 100 \mu$ m.

Then I tested the intermediate 1 nM/ μ m case and interestingly found that only cells very close to the aggregates (within $\sim 10 \mu$ m) migrated into them—the other individual cells bypassed the aggregates to chemotax up the gradient. This behavior qualitatively illustrated that, for the cells I was using, the chemotactic response of the cells increased when I increased the steepness of the gradient from 0.1 nM/ μ m to 1 nM/ μ m.

Quantitatively, all three gradients, cells move directionally up the gradient (figure 3.1 c-e). However, figure 3.4 shows that average speed more than triples in the 10 nM/ μ m case from the 0.1 and 1 nM/ μ m cases, countering the data from Song

et al. The standard deviation of angular displacement also decreased slightly from 0.1 to 1 nM/ μm (dropping from 31.56° to 10.75°), suggesting that a greater proportion of cells migrate directly up the gradient. Taken together, these analyses indicate at least that 1 and 10 nM/ μm gradient are more optimal for chemotaxis than 0.1 nM/ μm as previously published, and that 10 nM/ μm may be more optimal than 1 nM/ μm .

I thus chose 0.1, 1, and 10 nM/ μm gradient cases as my cAMP parameters so that I could test the effect of increasing cAMP gradient responses in my combination experiments. In the future, I will conduct follow-up Dunn assays at gradients of 10^{-2} and 10^2 nM/ μm , as well as determine the optimal level, lower limit, and upper limit of cAMP gradient detection in the cells I was using.

Second, I wanted to verify that cells could chemotax within my device at these gradients. As mentioned previously, flow is required to generate a gradient in the device, so I observed cells in gradients generated with low flow rates (experiencing shear stresses between 0.3 and 0.6 Pa) to cells in the same gradient in the Dunn chamber (Décavé *et al.*, 2003). I hypothesized that cells would chemotax in the microfluidic device at these chosen gradients, but that chemotaxis would be influenced by the shear stress caused by the flow used to generate the gradient. As expected, even low shear stresses had an effect—the angle of displacement shifted from directly vertical as compared to the Dunn chamber experiments. The nature of this shift is discussed in Combination Experiments, but for now the important observation to note is that cells were able to sense the chemical gradient because

the cells' angular displacements are restricted to the top two quadrants – i.e. always in the direction of increasing chemical concentration.

Combination Experiments

4. Cells integrate mechanical and chemical signals

After determining a range of shear stresses and cAMP gradients to test, I performed nine experiments, each experiment combining one of the three gradients and one of the three shear stress gradient regimes (0.3-0.6 Pa, 0.8-1.2 Pa, and 2.3-2.5 Pa—it was difficult to calibrate the shear stress to a specific value due to the imprecision of the vacuum regulator). Experiments in a particular column of figure 3.1 (g, l, p; h, m, q; i, n, r) were conducted in the same device with the same cells on the same day; data are from one trial. These experiments sought to address the overarching question of how cells behave when stimulated with both a chemical and a mechanical signal. I verified in Results sections 2 and 3 cells migrate in orthogonal directions in response. To reiterate, I hypothesized that in these combined conditions cells would either (1) respond to the two signals separately or (2) integrate the signals in some way.

In the first case, I would expect that displacement angles of individual cells would be clustered near 0° and 90° , with the number of points in each cluster dependent on the relative strength of each signal. In the second case, I would expect cell directions to be “diagonal,” with angular displacements falling between 0° and 90° .

The data in the angular displacement plots (figure 3.1g-i, l-n, p-r) favor the second hypothesis. Mean angular displacements lie clearly between 0° and 90° in the low and medium shear cases for all gradients and slightly above 0° in the high shear case, suggesting that while cells integrate the signal in some combination conditions, the mechanotactic component of movement is greater than the chemotactic component of at these stresses. I did observe that in the 0.1 nM/ μm /low shear and 10 nM/ μm /high shear cases, a few cells moved against the flow, indicating variability which I will discuss in Results section 7. Trends such as average displacement angle and standard deviation are also discussed subsequently.

5. Cells do not switch between chemotaxing and mechanotaxing under a combination of stimuli

After observing that cells move in a diagonal direction when stimulated with both signals, I considered that angular displacement I observed could occur in two ways: (1) cells could be moving in a diagonal manner or (2) cells could alternate between moving with flow and up the gradient, i.e. switching between responding to either separate signal. I watched the movies of cells and observed that cells that did were displaced diagonally appeared to *move* diagonally, rather than across and up, on the substrate. A representative set of cells tracks is shown for selected conditions in which cells are displaced diagonally in figure 3.5.

From the 5x magnification movies I could only determine that cells did not spend long periods in “chemotaxis” and “mechanotaxis” mode. However, I could not determine whether cells switched rapidly between the modes—for instance, did

cells take move up and across in small individual steps that are indiscernible in a lower-magnification time-lapse? This question was another motivation behind the higher magnification case discussed at the end of this section.

6. Changing the magnitude of shear stress changes the angle of displacement but changing the steepness of the cAMP gradient does not

I noticed from the displacement plots of the combined cases that the mean angle tended to shift towards 0° as shear stress increased. Figure 3.6, plotting mean angle against shear stress, confirms this trend in the data. This data suggests that at all three gradients, increasing the intensity of the shear stress signal increases the mechanotactic component of direction. One important note is that although mechanotaxis appears to overtake chemotaxis at high shear stresses in figure 3.1p-r, the mean displacement contains a small component of chemotactic response, i.e. the mean displacement angles are in the first quadrant. This may suggest that rather than switching to an alternate mode of migration at high shear stress, cells are still integrating the two signals but that the mechanotaxis signal is much stronger than the chemotactic signal.

I next asked whether changing the cAMP gradient would similarly affect cell behavior. Plotting mean angle against gradient (figure 3.7), I found that changing cAMP gradient has minimal impact on angle of displacement. The asterisk in figure 3.7 indicates the only point which was statistically significant. The kink in the low shear stress curve corresponds to the $1 \text{ nM}/\mu\text{m}$, low shear stress case and corresponds to a statistically different mean displacement angle from both the 0.1

nM/ μm , low shear case ($p=0.047$) and the 10 nM/ μm , low shear case ($p=0.0007$). However, the difference between the 0.1 nM/ μm case and the 10 nM/ μm case for low shear stress was statistically insignificant ($p=0.99$). All other comparisons of mean angle within a shear stress regime had $p>0.05$. This suggests that the 1 nM/ μm case is an anomaly and may simply be a result of the particular cells that were chosen for analysis—a larger number of analyzed cells and more trials will add statistical power to this conclusion. Taken together, these data seem to suggest that in this gradient range, the strength of the chemotactic signal does not affect the cell's ability to compete with mechanotaxis.

7. Cell-to-cell variability in direction decreases as shear stress is increased

I next asked what the relationship between the stimuli the cells experienced and the spread in their displacement was. Standard deviation is a reflection of cell-to-cell variability; each cell is different and cells in a population will express different behaviors when subjected to exactly the same stimulus because of differences in gene products. This variability has been characterized in *D. discoideum* (Samadani *et al.*, 2006).

I could not compare variances between gradient cases at a particular shear regime (i.e. low, medium, high) because (1) experiments were done at different shear stresses and in different devices, and (2) without repeated trials, I could not attribute differences to condition rather than trial-to-trial variability. However, I *could* compare cells in a particular gradient condition subjected to different shear

stresses because experiments were performed in the same device with the same set of cells.

Figure 3.8 plots standard deviation against shear stress and illustrates clearly that in all gradients, as shear stress increases, the standard deviation of angular displacement decreases. Thus cells with a larger mechanotactic component regime (towards 0°) exhibit less cell-to-cell variability. This phenomenon occurs in every gradient case. I considered the possibility that this striking conformity of displacement angle was due to some geometric phenomenon, such as aligning of the cell body due to flow, taken with the evidence average cell speed increases significantly at every shear stress. Thus higher-magnification imaging is important for elucidating phenomena occurring at the cytoskeletal level. In the Discussion section, I propose one way that this trend in variability may provide insight into the relationship between mechanotaxis and chemotaxis.

8. Cells may integrate mechanical and chemical signals at the pseudopod level

Some of the questions I had hoped to address with higher magnification time lapse movies were the following, reiterated from questions discussed throughout the rest of the results section: What sorts of phenomenon are occurring at the cytoskeletal level? Can any of them explain why cells move faster at higher shear stresses if they do not detach from the surface? For cells with a diagonal displacement, does the cell take very small steps up and across, thus switching between chemotaxis and mechanotaxis? Or is overall movement diagonal?

Due to limitations in availability of imaging equipment and time constraints, I was unable to carefully examine a variety of conditions under high magnification and resolution to answer these questions. I did, however, take a set of higher magnification (10x) time-lapse movies for low, medium, and high shear cases at 10 nM/ μ m. Although this data is preliminary, I was able to make some interesting observations. First, I did not observe cells alternate between horizontal and vertical movement—cells that moved diagonally appeared to take diagonal steps. Second, I observed two interesting phenomena involving pseudopods, shown in figure 3.9. In the first (a), a pseudopod that is oriented directly against the flow is retracted by the cell. In the second (b), a pseudopod oriented against the flow pivots around the adhered back edge of the cell and orients itself along the fluid flow. These phenomena may be crucial to understanding how cells integrate mechanical signals with chemical cues. It was very difficult to see cytoskeletal features with the resolution that was available, so in the future I would like to use better optics to more closely examine the mechanics of pseudopods at higher resolution, as well as study the dynamic localization of GFP-tagged actin within the cell because pseudopods are composed of polymerized actin.

IV. Discussion

Prior to this work, mechanotaxis and chemotaxis in *D. discoideum* had been studied separately but not simultaneously. In this work I subjected chemotaxis-competent *D. discoideum* cells to a spectrum of combined cAMP gradient and shear stress conditions. The key contribution of this study is evidence that when subjected to both shear stress and a cAMP gradient, *D. discoideum* cells react to both of the applied stimuli simultaneously. I observed that cells do not switch between chemotaxing and mechanotaxing—they integrate the two signals. In this section I address the question of where in the cell's signal processing machinery mechanotaxis and chemotaxis intersect and suggest they do not share an identical signaling pathway. Finally, I propose a mechanism by which cells mediate chemical and mechanical stimuli on the pseudopod level.

I hypothesized that I would observe experimental data matching one of the following models: (1) cells respond to either the chemotactic or mechanotactic signal, resulting in a population in which some cells moved in the direction of flow and others directly chemotaxed up the cAMP gradient; or (2) cells somehow integrated these signals and moved in a diagonal direction. I observed overwhelming evidence in favor of the latter model; at every cAMP gradient tested, all the cells in the population moved in a diagonal direction at low to medium shear stresses. From cell tracks I also determined that cells did not switch between chemotaxis and mechanotaxis strategies—cells with a diagonal angle of displacement did not spend significant periods moving directly horizontally or

vertically within the device. Taken together, these observations suggest that cells somehow integrate these two signals that, when applied independently, stimulate them to go in orthogonal directions.

I next sought to answer the question of *how* cells integrate these two signals. As mentioned in the Background section, a diagonal displacement shows that cells are responding to both the signals, but it does not reveal the nature of integration—for example, whether responses to chemotaxis and mechanotaxis are computed separately and superimposed, or rather if the signaling pathways of the two processes overlap. Décavé *et al.* (2003) suggest that chemotaxis and mechanotaxis share a PI3 kinase-dependent signaling pathway. The following three observations, however, strongly suggest that the chemotaxis and mechanotaxis mechanisms are in fact *separate* phenomena that do not share an identical molecular basis but rather are processed separately and superimposed.

First, mechanotaxis appears to be independent of the cAMP receptor. Cells moved directly in the direction of flow in both buffer (when none of the cAMP receptors were occupied) and in a uniform concentration of cAMP (when cAMP receptors were uniformly occupied), as well as in gradients of cAMP, at the same shear stress. In the future I plan to test a greater range of uniform cAMP concentrations to further explore the relationship between mechanotaxis and level of cAMP receptor-occupancy—for instance, will cells still mechanotax when receptors are completely saturated?

Second, cell-to-cell variability in angle of displacement decreases when cells are moving in a mechanotaxis regime rather than a chemotaxis regime within a

device. Individual cells in a population are putatively known to have different responses to a chemotactic gradient due to inherent differences in intracellular asymmetry and protein products (Samadani *et al.*, 2006). The chemotactic response has been modeled as the product of intracellular asymmetry and extracellular gradient. The observation that the same cells in a device are less variable under high shear stress implies that mechanotaxis is a separate process from chemotaxis—if the two shared the same molecular pathway, one would expect that behavioral variability would not be different under a mechanotaxis regime versus a chemotaxis regime.

Third, changing the magnitude of shear stress impacts the angle of displacement but changing the chemotactic gradient does not. As the steepness of the gradient is increased from 0.1 nM/ μ m to 1 nM/ μ m to 10 nM/ μ m at low and medium shear stresses, the average angle does not change significantly. One possible explanation is that increasing the steepness of the gradient does not change the ability of cells to “compete” with the mechanical signal. In other words, in the cAMP range tested, increasing the cAMP signal does not impact a cell’s direction of movement, but increasing the mechanical signal does. This seems to suggest that mechanical and chemical inputs are not computed together by the cell’s global signal processing system but rather processed separately and then added.

One contention to this last observation might be that in this range of gradients, the cells are “saturated”—that is, there is no improvement in chemotactic efficiency with increasing gradient. However, I observed that cells in a 0.1 nM/ μ m gradient in the Dunn chamber would migrate up the external gradient but then periodically

“switch” directions when in range of a pre-formed aggregation center releasing a natural cAMP relay wave. In a 1 nM/ μm gradient, the cells migrate up the external gradient and effectively ignore the aggregation centers. This seems to suggest that the cells are not saturated in a 0.1nM/ μm gradient and that increasing the steepness of the cAMP gradient does indeed increase the chemotactic response of the cells in the 1nM/ μm regime. Future studies to support this argument should include more finely sampling the possible range of gradients.

Follow-up experiment should include abrogating the cell’s PI3 kinase network and other proposed chemotaxis pathways to study whether mechanotaxis is reduced in developed cells as Décavé suggests it is in vegetative cells, which could provide counter-evidence to my claims that chemotaxis and mechanotaxis are separate from a signaling standpoint. Indeed, another possibility is that while mechanotaxis and chemotaxis do not share an identical signal transduction pathway, they may share some molecular components.

Finally, behavior can vary at the level of individual pseudopods, cells, or aggregates of cells. I propose that computation of the signals may occur at the pseudopod level rather than the cellular signal transduction level. I found evidence from three higher-resolution movies that cells respond to shear stress in two ways: (1) pivoting and (2) retraction of pseudopods. In the first mechanism, the backs of cells remain adhered to the substrate, and the rest of the cell body would then pivot around and align itself along the flow. This mechanism is dependent simply on the adhesiveness and geometry of the cell, which I will call the “pivoting mechanism.”

In the second mechanism, I observed that some pseudopods that are aligned opposite to the flow are actively retracted, and pseudopods aligned in the direction of flow are maintained. This selective mechanism, which I will term the “retraction mechanism,” is similar to the way that cells navigate shallow gradients of cAMP (Andrew and Insall, 2007). Cells continuously split pseudopods and maintain the pseudopods that sample cAMP higher concentrations while retracting pseudopods that sample lower concentrations. It would be interesting if this was indeed the mechanism by which cells mediate the two signals because in a case where a pseudopod which experiences a higher cAMP concentration is also oriented against flow the cell would have to “compute” the two signals and make a decision about whether to retract or maintain this pseudopod. To test this scenario, one could imagine an experiment in which a micropipette filled with cAMP was placed near a pseudopod, and a cantilever such as an atomic force microscope probed the same pseudopod with a mechanical force.

I propose that the cell responds to the mechanical signals through some combination of the pivoting and retraction mechanisms. This model is consistent with my earlier observations. First, the pseudopod-level computation of cell direction is downstream of the cAMP receptor. Second, cell-to-cell variability could be explained by this model because both pivoting and retraction could increase in concert with increased applied shear stress, causing more cells to migrate in the direction of shear flow. Third, it is consistent with the observation that cells do not change their angle of displacement under different gradient conditions but do under different stress conditions. Whether or not a “correct” pseudopod is picked under

the chemotaxis regime is independent of the steepness of the gradient. However, either pivoting or retraction or both may increase with increased shear stress. Finally, this model is consistent with the observation that cells move out of aggregates when stimulated with external cAMP but not when stimulated with mechanical stress. Cells near the edge of the aggregate experiencing shear stress will not pick pseudopods at that edge. Cells away from stress will be shielded from the shear stress and thus have no incentive to move from the aggregation center.

At this point in experimentation, however, this model remains speculative. Future work will include more trials, analyzing a larger number of cells, and exploring more experimental parameters. I first hope to repeat experiments at a higher magnification. At a better imaging resolution, I can be more confident of my observation of pseudopod pivoting and retraction. I also plan to do a more rigorous image analysis of these higher-resolution movies to determine the ratio of cell pivots to pseudopod retractions at a given shear stress and cAMP gradient.

Second, in order to distinguish between the possibilities that (1) more pseudopods are generated in the direction opposite to flow, as proposed by Décavé *et al.* and (2) fewer pseudopods are retracted in the direction opposite to flow, I plan to take high-resolution fluorescence movies of cells with GFP-tagged actin. If indeed cells are generating more pseudopods in the side of the cell opposite to flow, I would expect to see greater actin enrichment at this side of the cell. This analysis would also distinguish between an “instructive” and “selective” model of cell decision making. In the former, a signal such as chemical or mechanical stress instructs a cell to make more pseudopods in the appropriate direction. In the latter,

the cell explores the space with several different protrusions that are equally likely to be maintained unless selected with a larger probability by some signal.

Third, I would like to explore the effect that making a cell more adhesive has on the pivoting mechanism. Ca^{2+} , for instance, makes cells adhere more strongly to substrates, so it would be interesting to observe (1) if pivoting still occurs and if so, (2) if pivoting decreases, then will the retraction mechanism predominate? Will retraction be enough to shift the angle of cell displacement? Will cell-to-cell variability at high shear stress increase?

The exploratory nature of my project generates novel and interesting questions and provides emerging insight into how *D. discoideum* mediates chemical and mechanical signals. More intriguingly, this data could eventually provides clues about how other eukaryotic cell types such as neutrophils, cancer cells, and germ cells navigate complex mechanical and chemical environments.

V. Materials and Methods

Media and growth conditions

Act-15 GFP-tagged (strain AX3) *Dictyostelium discoideum* cells were cultured in 5 mL of HL-5 medium (56 mM glucose, 10 g/L peptic peptone, 5 g/L yeast extract, 2.5 mM Na₂HPO₄, 2.6 mM KH₂PO₄, pH 6.5) at 25°C in 100 mm Petri dishes. Cells were passaged using sterile technique every other day to maintain at approximately 10⁷ cells/mL.

Cell development and preparation

Sub-confluent plates of cells (10⁷ cells/mL) grown in HL5 were washed with KK₂ buffer (2.2 g/L KH₂PO₄, 0.7 g/L K₂HPO₄) and resuspended in 10% HL5 solution (0.5 mL HL5 medium, 4.5 mL KK₂ buffer) to induce the developed stage. After 12-16 hours, developed cells were washed in KK₂ buffer and re-suspended to a final concentration of 2 x 10⁶ cells/mL. Cells were filtered through a 40 µm filter to eliminate large aggregates before loading.

Dunn chamber assay

The inner well of the DCC100 Dunn chamber (Hawksley, Lancing, Sussex, BN) was filled with 50 µL of KK₂ buffer. A 1-mL droplet of cells (2 x 10⁶ cells/mL) was seeded onto a Dunn cover slip and allowed to adhere for 30 minutes. Excess liquid was wicked off of the cover slip with a tissue, and the cover slip was gently inverted over the central well of the chamber with a small gap between the edge of the well and the cover slip. Excess fluid around the cover slip was wicked off, and 70 µL of the appropriate cAMP concentration was pipetted into the outer well. To make a 10 nM/µm cAMP gradient, a 10 µM solution of 98.0% adenosine 3',5'-cyclic monophosphate powder (Sigma Aldrich) suspended in KK₂ was used as the source because the two wells were separated by 1 mm. The gradient between source of cAMP (outer well) and sink of buffer (inner well) was established by diffusion after 20 minutes. Cells adhered on the cover slip between the inner and outer wells were imaged. One trial was conducted for each Dunn assay.

Master design and fabrication

The overall assembled microfluidic device consists of a polydimethylsiloxane (PDMS) block bonded to a glass slide. The device design was a gift from Jagesh Shah (Harvard Medical School, Boston, MA) and was printed on a transparent plastic sheet to create a mask.

Standard photolithography methods were used to create the master, or the

template, for the device. All microfabrication procedures were done in the clean room in the Harvard Medical School Goldenson building. 10 mL of SU-8 2025 negative photoresist (Microchem, Newton, MA) was poured onto Si wafers. The wafer was spin coated with SU-8 at 2500 rpm. The wafer was baked for 5 minutes at 65^oF, 2 minutes at 75^oF, and 6 minutes at 95^oF. The mask was overlaid on the master, and the master was exposed with UV light for 18 seconds using a Suss MJB mask aligner (Suss MicroTec, Garching, Germany). The masters were baked for 3 minutes at 65^o F and then for 6 minutes at 95^oF. Wafers were then submerged in SU-8 developing solution (Microchem, Newton, MA) and washed with isopropanol and distilled water. Wafers were baked at 150^oF for 2 hours. Photoresist on the exposed portions of the master were cross-linked by exposure to UV light. Thus, when submerged in SU-8 developer, the non-cross-linked parts of the mask are etched away, leaving a pattern of hardened SU-8 that serves as a template for device fabrication.

Microfluidic device fabrication

40 g of Sylgard 184 silicone elastomer base (Dow Corning Corp., Midland, MI) was mixed with 8 g of Sylgard 184 silicone elastomer curing agent (Dow Corning Corp., Midland, MI) and degassed using a centrifugal mixer (Thinky USA Corp., Tokyo, Japan). This mixture of elastomer (PDMS) was poured over the wafer in an aluminum foil cup. Foil cups were put in a vacuum chamber for 1-2 hours to allow further degassing of the PDMS. The elastomer was baked at 65^oF for 30 minutes to allow the mixture to harden. Foil was then peeled off the hardened PDMS.

Individual devices were cut from the PDMS block. A 0.75 mm biopsy punch (Harris Uni-Core, Redding, CA) was used to punch a hole at inlets 1-4. The device was washed with isopropanol before plasma etching.

To finish assembling the device, PDMS blocks and microscope slides were etched for 15 seconds at 115 W at 100 mTorr in a Plasma Technics 500-II plasma etcher (Street Racine, WI). Devices were immediately assembled by gently pressing the patterned face of the PDMS blocks onto the glass slides. Devices were baked for 10 minutes at 90^oF.

Microfluidic assay

Please see protocol development for cell loading procedures. Tubing of radius 0.02 inches was used to connect inputs and outputs to the device. cAMP was purchased as solid powder from Sigma Aldrich at 95% purity.

After cell loading, 60 minute movies were taken. In gradient/shear stress combined experiments, the gradient was established first at low flow, and the cells adjusted to the gradient. After chemotaxis was observed (after approximately 20 minutes), the shear stress was turned up to the experimental condition.

Videomicroscopy

All time-lapse recordings were made using a Zeiss Axiovert 100 inverted microscope and a FAST Mono-12bit QICAM digital camera. 5x recordings used a DIC filter and were acquired at a sampling rate of 6 images/ minute. 10x recording used a phase contrast filter and were acquired at a sampling rate of 12 images/ minute. Images were acquired using MetaMorph software.

Image analysis

Image analysis was performed using Image J analysis software. Cells were picked randomly from a frame in the middle of the 60-minute time lapse (after typically 20 minutes) and followed frame to frame for 20-40 minutes. Tracking was stopped when cells that stopped moving abruptly, or touched another cell during imaging,

Due to time constraints, only 10-20 cells were analyzed per movie. However, appendix figures A.1 and A.2 show an alternate method of measuring cell angular displacement, in which consecutive frames are collapsed and angular displacements are measured by measuring the angle between the start point and end point. This method of analysis was conducted for 30 cells.

Statistics

Statistics were conducted on angle of displacement using a pair-wise Watson-Williams F-test, which compares two mean angles to determine if they differ significantly. A p-value below 0.05 was considered significant.

References

- Andrew, N., and Insall, R.H. (2007). Chemotaxis in shallow gradients is mediated independently of PtdIns 3-kinase by biased choices between random protrusions. *Nat Cell Biol* 9, 193-200.
- Bagorda, A., and Parent, C.A. (2006). Eukaryotic chemotaxis at a glance. *J Cell Sci* 121, 2621-2624.
- H. C. Berg and P. M. Tedesco. Transient response to chemotactic stimuli in *Escherichia coli*. *PNAS*, 72(8):3235–3239, 1975.
- Bosgraaf, L., and Van Haastert, P.J.M. (2009a). Navigation of Chemotactic Cells by Parallel Signaling to Pseudopod Persistence and Orientation. *PLoS ONE* 4, e6842.
- Bosgraaf, L., and Van Haastert, P.J.M. (2009b). The ordered extension of pseudopodia by amoeboid cell in the absence of external cues. *PLoS ONE* 4, e5253.
- Bourne, H.R., and Weiner, O. (2002). A chemical compass. *Nature* 149, 21.
- Décavé, E., Garrivier, D., Bréchet, Y., Fourcade, B., and Bruckert, F. (2002). Shear flow-induced detachment kinetics of *Dictyostelium discoideum* cells from solid substrate. *Biophys J* 82, 2383-2395.
- Décavé, E., Rieu, D., Dalous, J., Fache, S., Brechet, Y., Fourcade, B., Satre, M., and Bruckert, F. (2003). Shear flow-induced motility of *Dictyostelium discoideum* cells on solid substrate. *J Cell Sci* 116, 4331-4343.
- Discher, D.E., Janmey, P., and Wang, Y. (2005). Tissue cells feel and respond to the stiffness of their substrate. *Science* 310, 1139-1143.
- Jannat, R.A., Robbins, G.P., Ricart, B.G., Dembo, M., and Hammer, D.A. (2010). Neutrophil adhesion and chemotaxis depend on substrate mechanics. *J Phys: Condens Matter* 22.
- Jeon, N.L., Baskaran, S.K., Whitesides, G.M., Van de Water, L., Toner, M. (2002). Neutrophil chemotaxis in linear and complex gradients of interleukin-8 formed in a microfabricated device. *Nature Biotech* 20, 826-830.
- Kessin, R.H. *Dictyostelium: Evolution, Cell Biology, and the Development of Multicellularity*. Cambridge University Press: Cambridge, 2001.

- King, J.S., and Insall, R.H. (2009). Chemotaxis: finding the way forward with *Dictyostelium*. *Trends in Cell Bio* 19(10), 523-530.
- Parent, C.A., and Devreotes, P.N. (1999). A cell's sense of direction. *Science* 284, 765-769.
- Samadani, A., Mettetal, J., and van Oudenaarden, A. (2006). Cellular asymmetry and individuality in directional sensing. *PNAS* 103, 11549-11554.
- Satulovsky, J., Lui, R., and Wang, Y. (2008). Exploring the control circuit of cell migration by mathematical modeling. *Biophys J* 94, 3671-3683.
- Song, L., Nadkarni, S.M., Bodeker, H.U., Beta, C., Bae, A., Franck, C., Rappel, W., Loomis, W.F., Bodenschatz, E. (2006). *Dictyostelium discoideum* chemotaxis: threshold for directed motion. *Euro J Cell Bio* 85, 981-989.
- Van Haastert, P.J.M. (2010). Chemotaxis: insights from the extending pseudopod. *J Cell Sci* 123, 3031-3037.
- Wang, L., Liu, D., Wang, B., Sun, J., and Li, L. (2008). Design of parallel microfluidic gradient-generating networks for studying cellular response to chemical stimuli. *Front Chem China* 3, 384-390.
- Wang, N., Tytell, J.D., and Ingber, D.E. (2009). Mechanotransduction at a distance: mechanically coupling the extracellular matrix with the nucleus. *Nature Reviews Mol Cell Bio* 10, 75-82.
- Wang, L., Liu, D., Wang, B., Sun, J., and Li, L. (2008). Design of parallel microfluidic gradient-generating networks for studying cellular response to chemical stimuli. *Front Chem China* 3(4), 384-390.
- Zicha, D., Dunn, G.A., and Brown, A.F. (1991). A new direct-viewing chemotaxis chamber. *J Cell Sci* 99(4), 769-775.

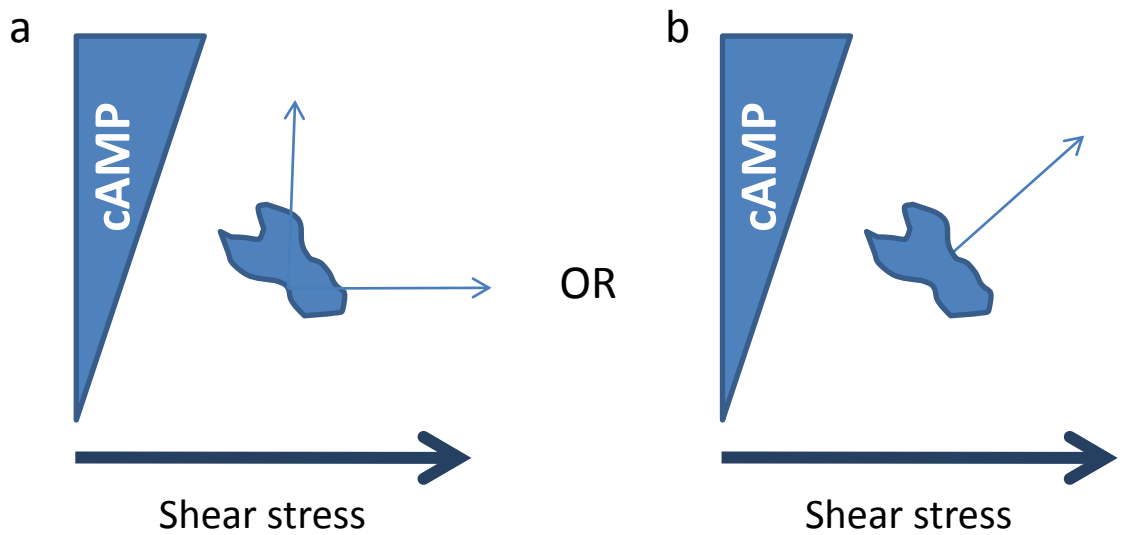


Figure 1.1 | Alternate hypotheses about cellular response to simultaneous chemical and mechanical signals

a. Cells respond to either the chemical or the mechanical signal, based on the relative magnitudes of each signal. Cells will either move directly right (in response to the force due to shear stress) or directly up (in response to the chemotactic signal).

b. Cells respond to both the chemical and the mechanical signal by moving in some diagonal direction. It is important to note that a diagonal direction indicates that the cell is responding to both signals simultaneously, but not whether (1) the cell simply superimposes the signals or (2) a more complex integration is occurring through the signal processing machinery of the cell.

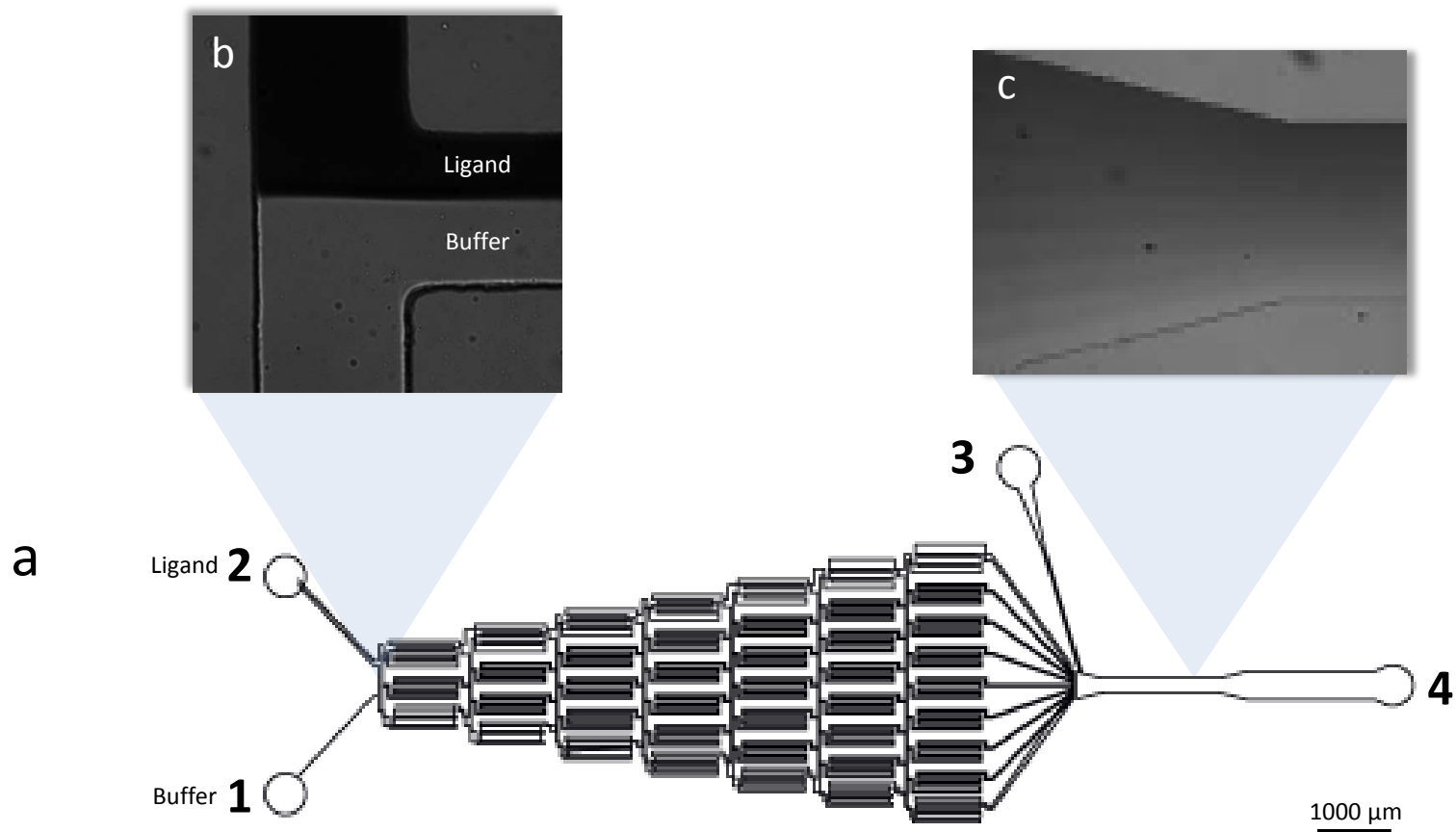


Figure 2.1 | Pyramidal microfluidic gradient generator

a. This microfluidic gradient generator with four inlets (a gift from Dr. Jagesh Shah, Harvard Medical School), relies on a hierarchy of serpentine microchannels downstream of inlet 1 (buffer input) and inlet 2 (ligand input). Two fluid streams converge to three output channels. Due to laminar flow, one channel is pure buffer, one channel is pure ligand, and the central channel is split into equal streams of ligand and buffer, as shown in **b** (inset). Diffusive mixing is facilitated by the length of the channels and the folding geometry at the corners. This effect is amplified through the levels of the device so that the output of the network is a series of parallel streams of fluid with ratiometrically decreasing concentrations of cAMP, as shown in **c** (inset). Downstream, in the cell chamber, the parallel streams mix diffusively to create a smooth gradient profile. Cells are loaded in inlet 4 and pulled into the cell chamber through negative pressure at inlet 3.

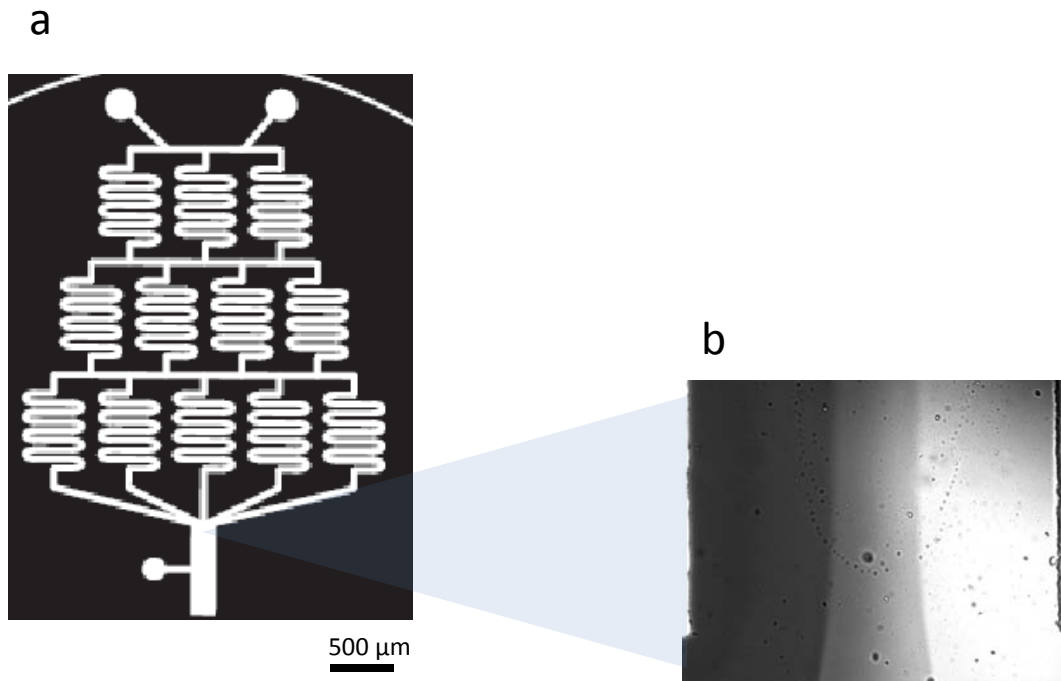


Figure 2.2 | First attempt at generating a microfluidic gradient

a. This device design failed because there were too few levels in the hierarchy, the channels were too short to allow proper diffusive mixing, and the cell chamber was too short to allow a smooth concentration gradient to be formed. The result, shown in **b** (inset) was a "stepped," rather than a smooth concentration profile in the cell chamber, imaged with blue food coloring.

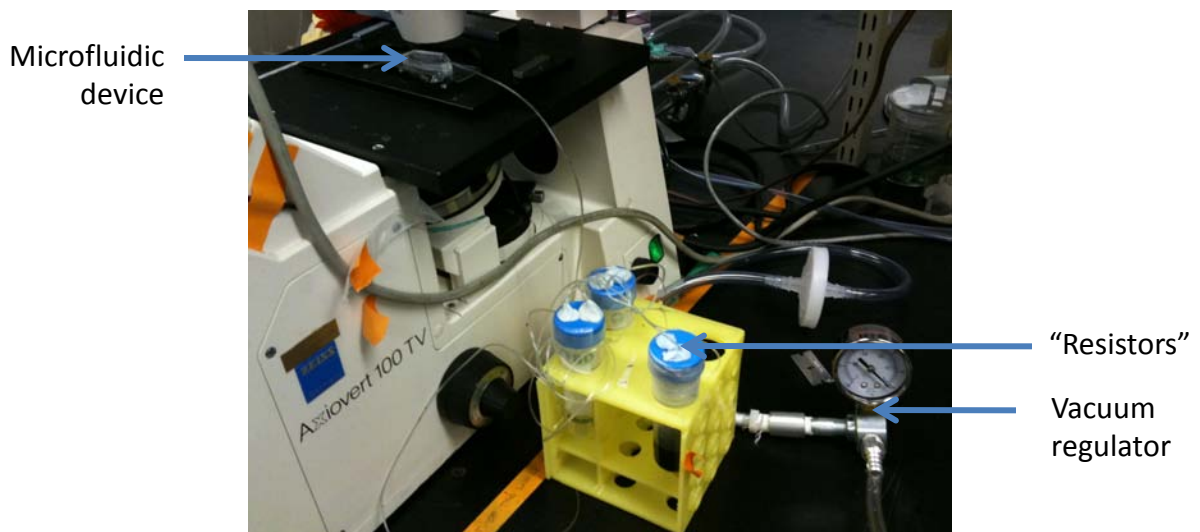


Figure 2.3 | Setup of the experimental platform used for microfluidic assays

a. This platform consisted of a microfluidic device mounted on a microscope slide for viewing. Inlet 4 of the device is connected with plastic tubing to a series of resistors made from 10 mL plastic tubes sealed with parafilm. Downstream of the resistors is a vacuum regulator that allows modulation of the vacuum level.

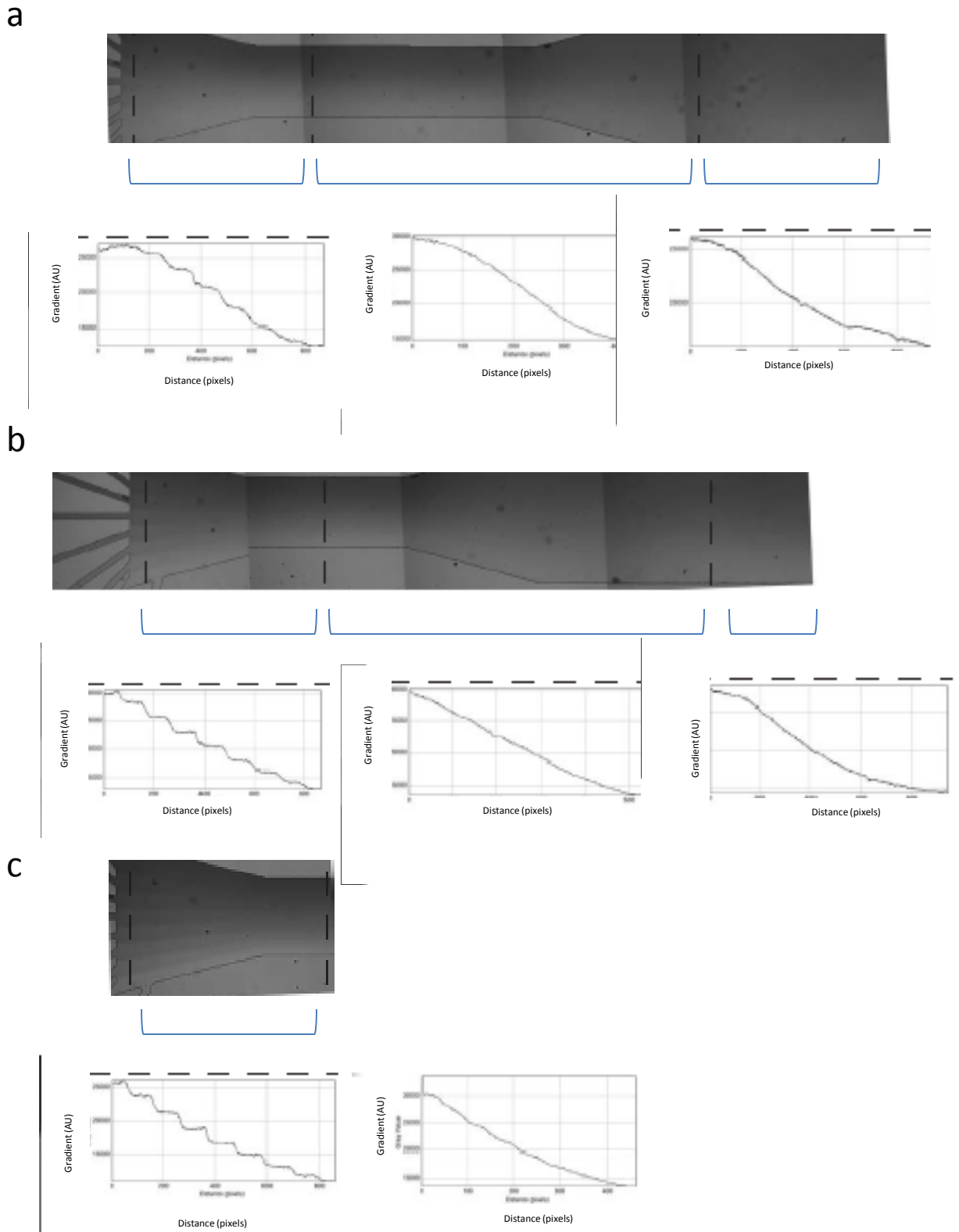
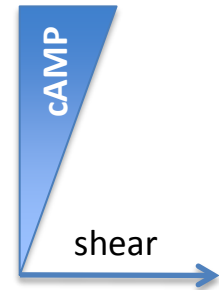
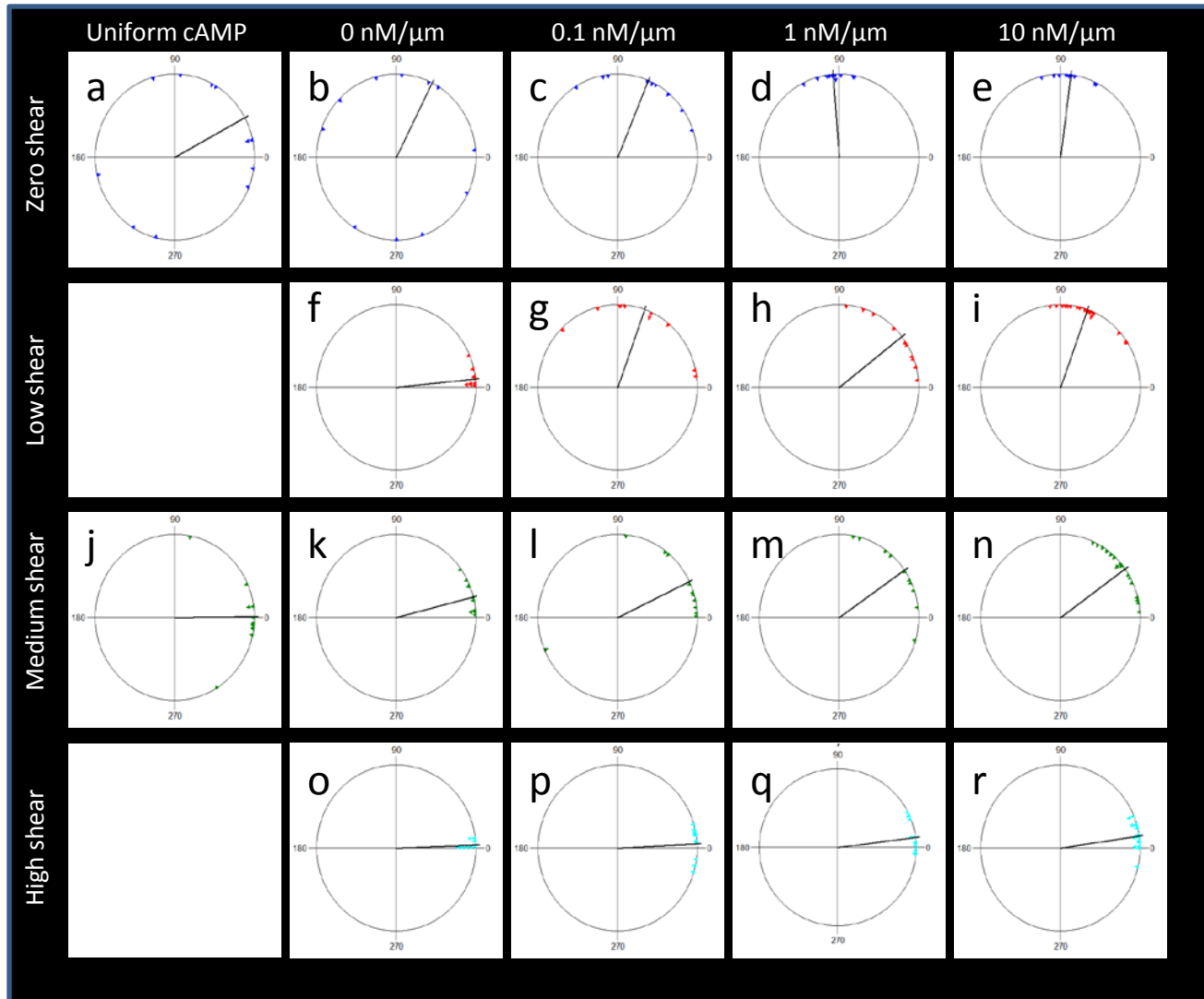


Figure 2.4| Concentration profiles across the cell chamber

(a-c). Food dye (dark) and buffer (light) were used to determine the effect of increasing vacuum pressure on the stability of the gradient. The results show that even as high as 16 psi (c), the gradient is smooth in the cell chamber. A stepped profile is apparent at the output of the network. Profiles created using Image J image analysis software. In the profiles, a high pixel intensity corresponds to a low arbitrary unit of gradient (AU).

Figure 3.1| *D. discoideum* integrate chemical and mechanical signals



Displacement angles of cells in different cAMP and shear conditions are shown. Cells stimulated with combined gradient and shear conditions exhibit a diagonal angular displacement rather than clustering at the 0° and 90° poles, suggesting that cells integrate signals rather than responding to a one separate stimulus.

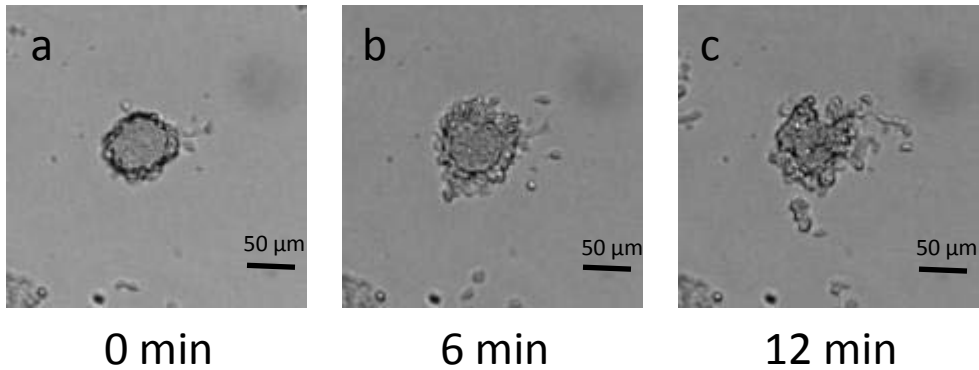
Points along the unit circle denote raw data. The black bar on each circular graph indicates mean angular displacement.

Table 3.1 | Summary of experiments

Subfigure	Shear stress (± 0.1 Pa)	n cells	Mean angle	SD
a	0	11	28.35°	88.74°
b	0	11	63.42°	109.11°
c	0	9	67.67°	31.56°
d	0	10	94.2°	10.75°
e	0	10	82.69°	11.90°
f*	0.4	10	5.94°	6.80°
g**	0.3	10	70.26°	37.80°
h***	0.6	19	38.11°	25.57°
i****	0.6	10	70.39°	17.68°
j	1.2	11	0.76°	30.06°
k*	0.8	10	14.39°	10.96°
l**	0.8	11	25.72°	45.33°
m***	1.2	10	34.94°	28.50°
n****	1.3	17	36.07°	18.42°
o*	2	8	2.122°	2.82°
p**	2.4	10	2.79°	10.94°
q***	2.3	11	352.83°	11.36°
r****	2.5	15	8.39°	9.44°

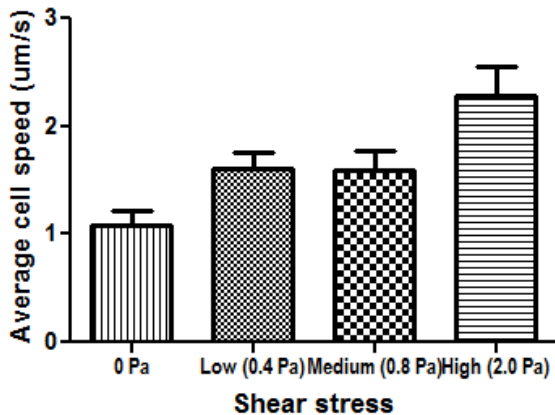
Shear stress values, number of cells analyzed, mean angular displacement, and circular standard deviation of means for each trial corresponding to figure 3.1a-r. One trial was conducted for each set of conditions. (*), (**), (***), and (****) denote trials that were conducted in the same device with the same cells. N cells in a time-lapse movie were selected at random for analysis. The center of mass of each cell was tracked for at least 20 minutes (120 frames every 10s). Mean angle was computed by computing $\arccos(X)$, where X= x-component of displacement/total displacement.

Figure 3.2 | Cells migrate out of aggregates in the presence of external cAMP



(a-c). In a uniform solution of 1 μM cAMP in the device, cells move out of aggregates, possibly due to an accidental gradient set up between the edges and center of the aggregate). The same phenomenon was observed in cells in uniform cAMP at medium shear.

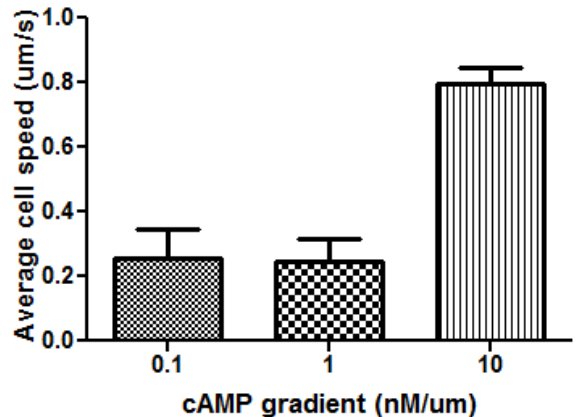
Figure 3.3 | Average speed of cells in buffer with varying shear stress



Relationship between average speed and shear stress in cells in buffer. Average cell speed increases with increasing shear stress, but cells did not detach from the surface. High-magnification imaging may help resolve why and how cells move faster under high shear stress.

The zero pressure case consists of cells moving randomly in buffer. Low, medium, and high shear stress experiments are from the same set of cells in the same device. Shown are average cell speeds with +SE measurements. One trial was conducted for each condition. Speed= total distance/time

Figure 3.4 | Average cell speed in Dunn chamber assays



Relationship between average speed and cAMP gradient in the absence of flow in a Dunn chamber. Average cell speed increases dramatically at 10 $\text{nM}/\mu\text{m}$. Taken with the directional movement of cells up the gradient, this may indicate that this gradient induces a more efficient chemotactic response than the shallower gradients tested.

Shown are average cell speeds with +SE measurements. One trial was conducted for each condition.

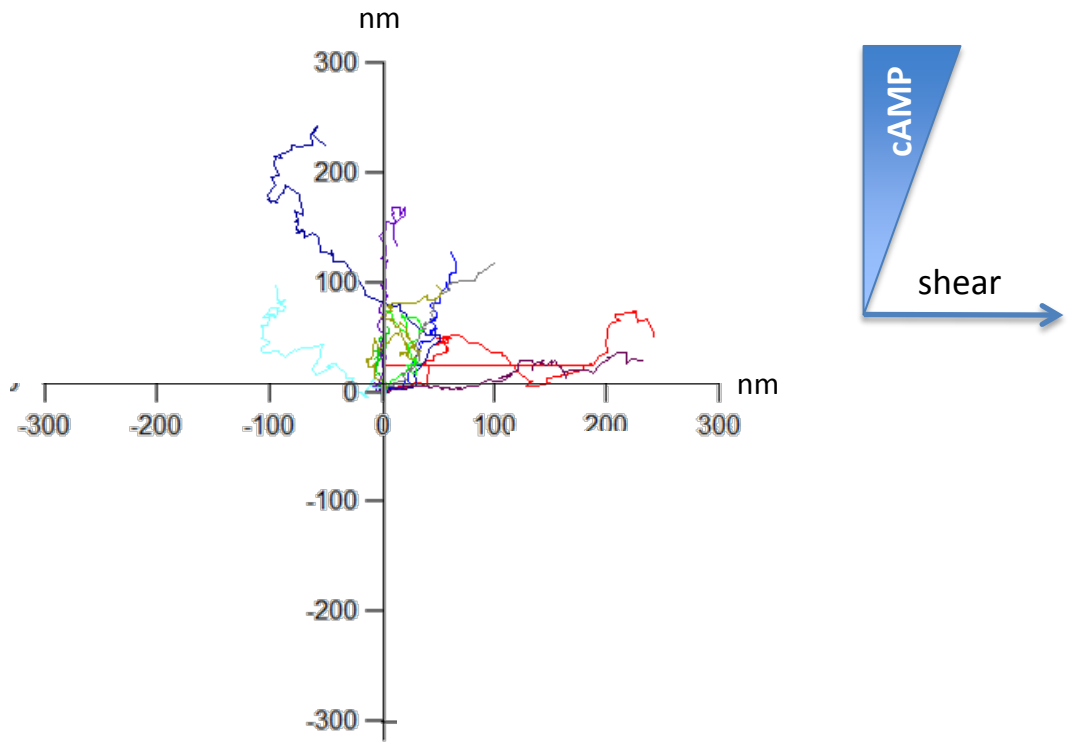
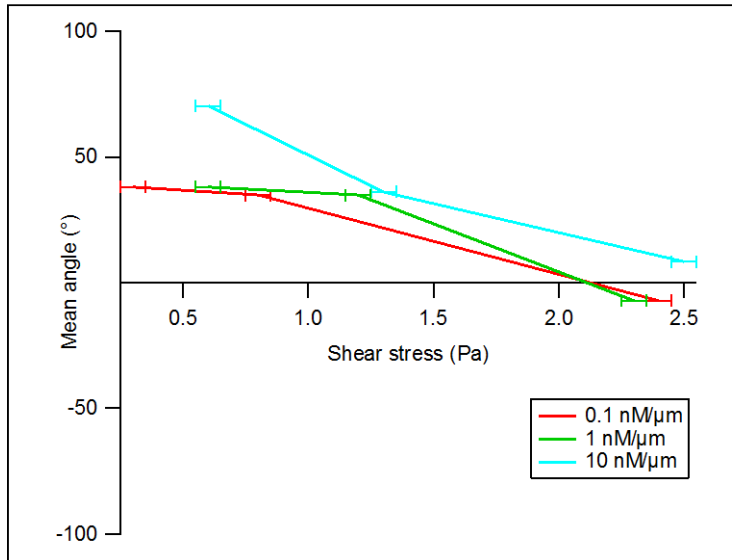


Figure 3.5 | Representative cell tracks show that cells do not switch between chemotaxis and mechanotaxis

Cell tracks are shown for cells in $0.1 \text{ nM}/\mu\text{m}$ case under low shear stress ($0.4 \pm 0.1 \text{ Pa}$). Cells that move diagonally do not appear to exhibit a stair-step pattern of movement that would indicate switching between chemotaxis and mechanotaxis. Zig-zag movement on a very small cannot be resolved with the 5x magnification movies that were taken.

Cells were analyzed for 32 min movies with a sampling rate of 10s/frame. The center of mass of each cell was manually selected in each frame. The starting positions of each cell was brought to the origin by subtracting the position of the first point from all subsequent positions, and the position of the cell was plotted over time. Each cell is represented by a different color.

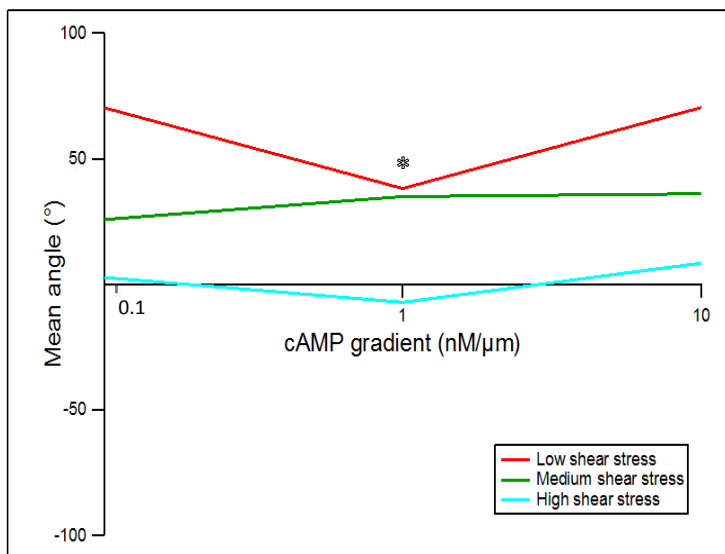
Figure 3.6 | Changing the magnitude of shear stress changes angle of displacement



The relationship between mean angle and shear stress for the three gradient conditions. Angle of displacement decreases with shear stress in each gradient condition, suggesting that increasing the intensity of the shear stress signal increases the mechanotactic component of direction.

Error bars indicate the ± 0.1 Pa error in shear stress.

Figure 3.7 | Changing the magnitude of cAMP gradient does not change angle of displacement



The relationship between mean angle and cAMP gradient for the three stress regimes. Angle of displacement does not change significantly as cAMP gradient is changed ($p > 0.05$) for the medium and high shear cases. Taken with the earlier observation that chemotactic efficiency increases with gradient steepness in the gradient ranges tested, this suggests that mechanotaxis and chemotaxis do not “compete” based on signal intensity.

The * indicates a significantly different measurement of mean angle in the low shear case between 1 nM/μm and 0.1 nM/μm, 10 nM/μm, respectively ($p = .047$ and 0.0007). However, this is likely an anomaly because the difference in mean angle between 0.1 nM/μm and 1 nM/μm case is insignificant ($p = 0.99$).

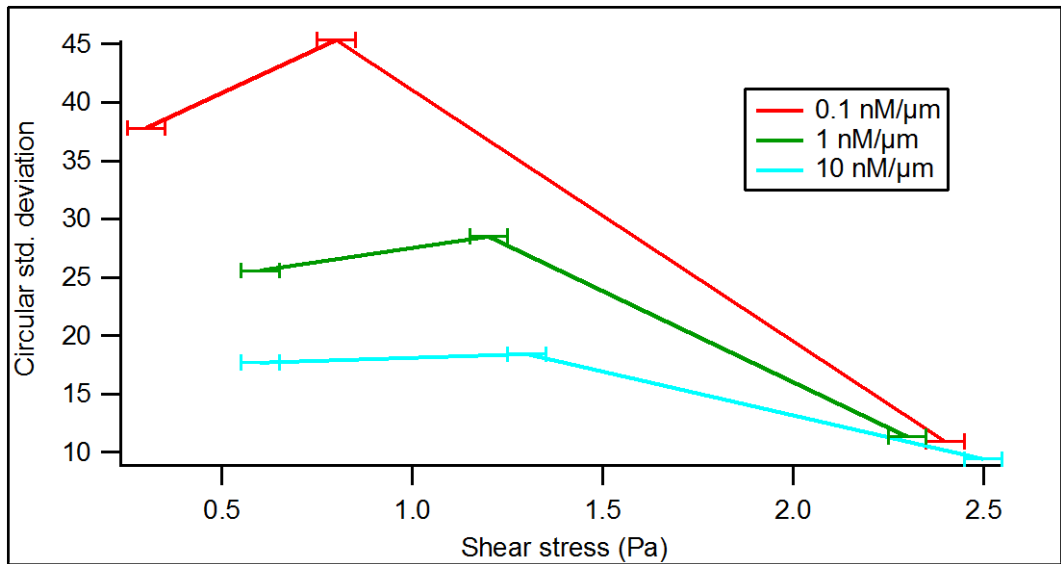


Figure 3.8 | Circular standard deviation decreases with shear stress

In all three gradient cases, the circular standard deviation decreases with shear stress. This result may be an indication that mechanotaxis and chemotaxis are separate phenomena rather than signal processed together.

Error bar ± 1 SD of shear stress.

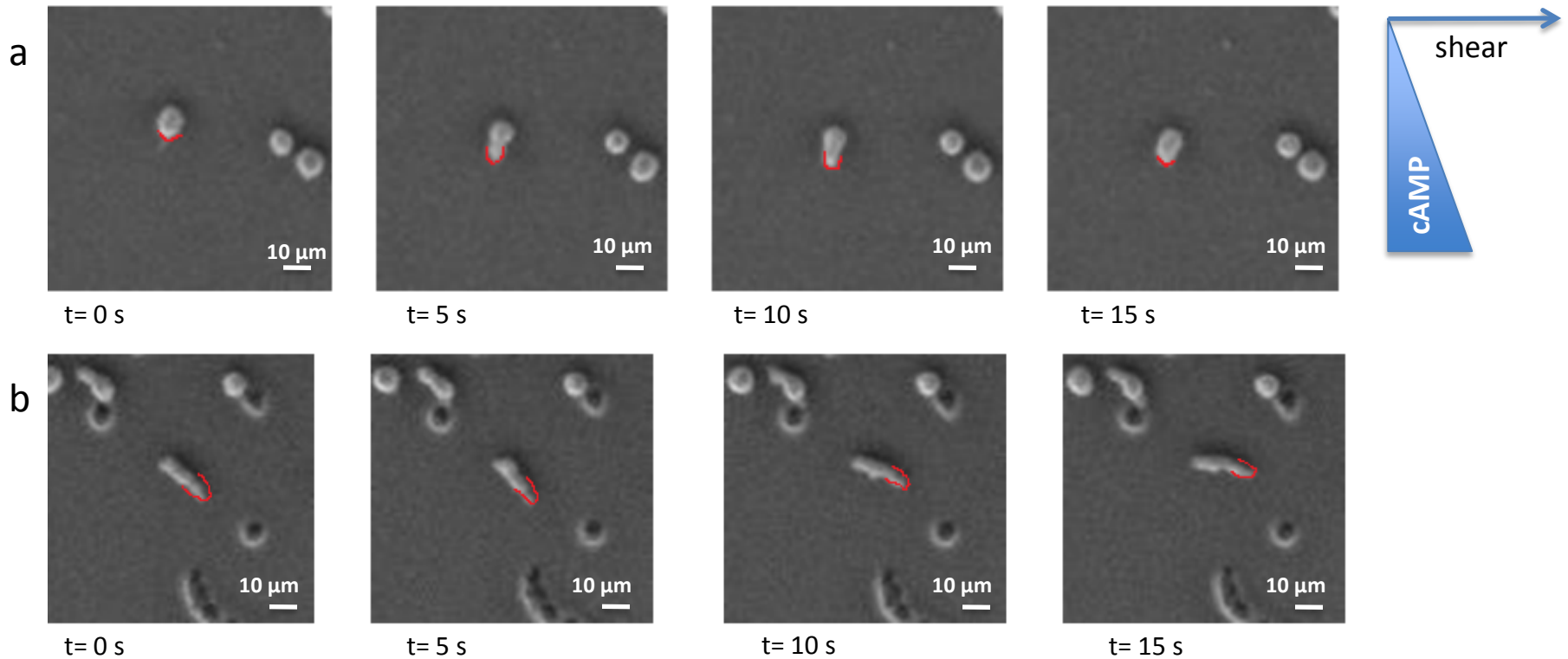
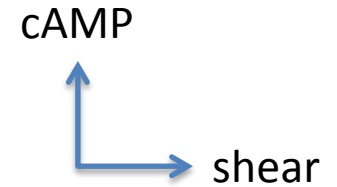
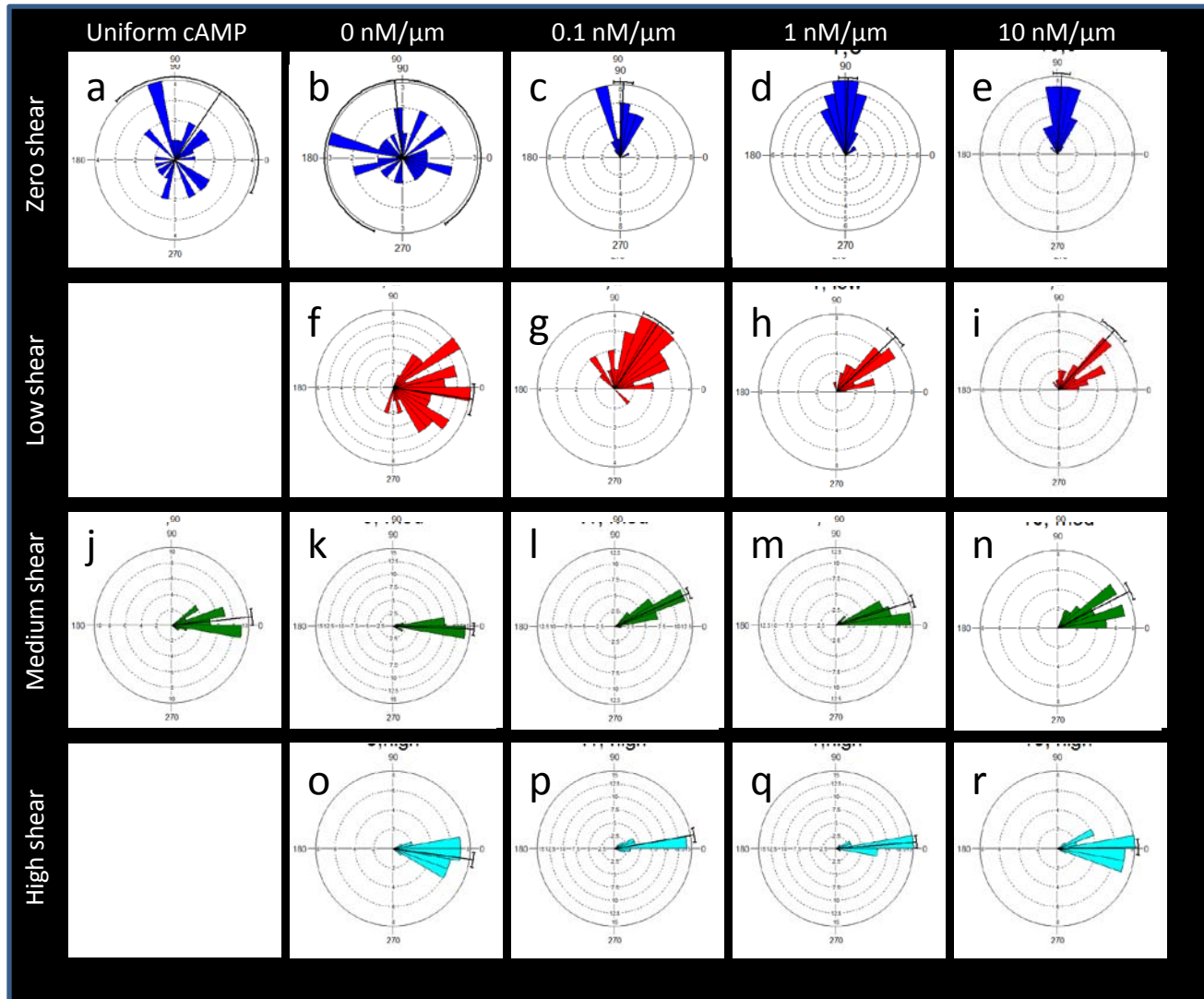


Figure 3.9| Retraction and pivoting of pseudopods

Possible mechanisms of ways that cells process mechanical signals. **(a)** A pseudopod oriented in the face of flow is retracted, consistent with a selective retraction mechanism. **(b)** A long pseudopod detaches from the substrate and pivots on the adhered back edge of the cell to orient itself in the direction of flow, consistent with a pivoting mechanism. It is possible that cells respond to the mechanical signal using a combination of these two mechanisms.

Images are 10x phase contrast. Experiment is the 10 nM/ μ m, low shear case. Pseudopods are outlined in red.

Figure A.1 | Histogram of *D. discoideum* Displacements



Here is used an alternate method of measuring angular displacement that is less rigorous than tracking the center mass of each cell in each frame. I used the Image J Z-project function to collapse 30 images into a single picture (5 minutes of data) and measured the angle between the start and end points. This circular histogram represents another method of verifying trends in angular displacements by giving the general direction that the cells travel in a *short* amount of time. It also reflects higher sample values and shows similar trends with the raw data in figure 3.1

Bands represent 10^0 bins . Number in each bin is indicated on the graph. The bar is mean angle of displacement. 30 cells from each case are analyzed.

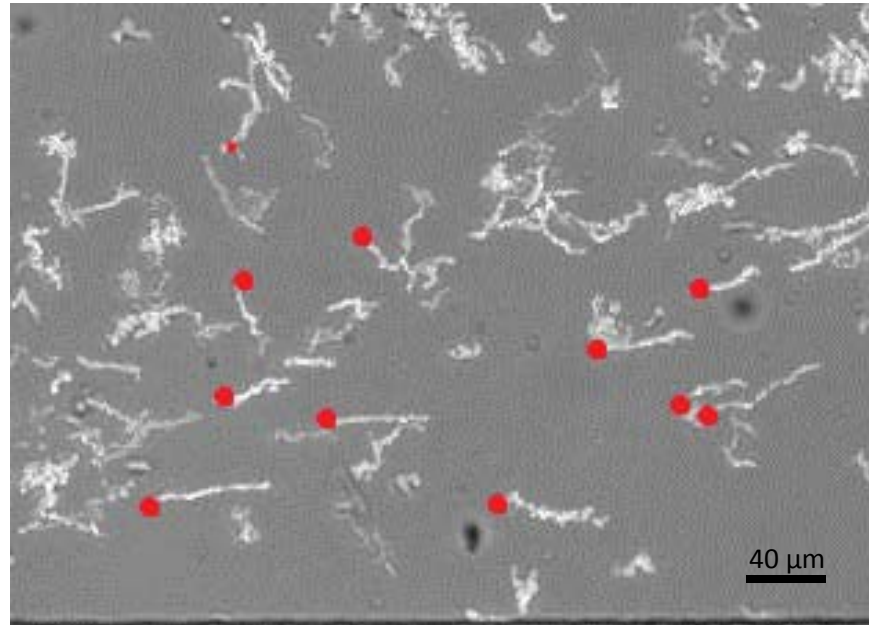


Figure A.2 | Z-projection of cell tracks

This z-projection, created in Image J, shows 5 minutes of images projected into one image for the medium shear stress and 1 nM/ μm). The red dots signify the starting position of cells.

Image taken with 5x magnification, DIC microscopy.